SC-RR-72-517

D-5

UC-35

Research Report

SC-RR-72 0517

AIRBLAST FROM SEQUENCED EXPLOSIONS OF CHARGES HORIZONTALLY DISPERSED IN THREE VERTICAL LAYERS

L. J. Vortman
Underground Physics Division

Printed October 1972

SANDIA LABORATORIES

OPERATED FOR THE UNITED STATES ATOMIC ENERGY COMMISSION BY SANDIA CORPORATION | ALBUQUERQUE, NEW MEXICO, LIVERMORE, CALIFORNIA

Issued by Sandia Laboratories,
a prime contractor to the United States Atomic Energy Commission

---

Printed in the United States of America

Available from
National Technical Information Service
U.S. Department of Commerce
5285 Port Royal Road
Springfield, Virginia 22151
Price: Printed Copy $3.00; Microfiche $0.95

SC-RR-72 0517

AIRBLAST FROM SEQUENCED EXPLOSIONS OF CHARGES HORIZONTALLY DISPERSED IN THREE VERTICAL LAYERS

L. J. Vortman
Underground Physics Division 9111
Sandia Laboratories
Albuquerque, New Mexico
87115

October 1972

ABSTRACT

Airblast was measured at distances of 2000 to 61,000 feet from a detonation of four million pounds of ammonium nitrate. The charge was horizontally dispersed in three vertical layers. The top layer contained 0.596 million pounds; the second, 160 feet below, contained 2.119 million pounds and was detonated 87 msec after the first; the third, 100 feet below the second, had 1.285 million pounds and was detonated 144 msec after the first. Attempts to reproduce measured ground-shock-induced peak overpressure using results of previous single, row, and array-charge explosions showed best agreement with the equivalent row-charge analogy, which produced 80 percent of measured values.

Key words: Airblast and explosion of dispersed charges

ACKNOWLEDGMENTS

Airblast measurements were made by J. R. Dickinson, assisted by C. B. Taft and G. L. Wright. R. J. Beyatte and G. L. Riggins were responsible for data playback and digitizing. J. W. Long prepared the adjusted records displayed in the Appendix.

AIRBLAST FROM SEQUENCED EXPLOSIONS OF CHARGES HORIZONTALLY DISPERSED IN THREE VERTICAL LAYERS

INTRODUCTION AND BACKGROUND

Recognition of airblast as a damaging explosion mechanism led during World War II to intensive study of airblast produced by bombs and chemical explosives.[1] Development of nuclear weapons extended the scope of the study.[2] Use of chemical and nuclear explosives underground led to examination of airblast from buried explosions for both military and Plowshare purposes.[3-5]

In most applications, the use of explosives involves the consideration of safety to nearby facilities, and safety assessment depends on an understanding of airblast from a wide variety of explosive applications. Understanding as it exists today results from studies of airblast from such diverse sources as underground nuclear testing, mining activities, and sonic booms.

Mathematical and physical models have been developed for at least two cases:

1. Point source explosions of HE[6] or NE[7-10] in a homogeneous atmosphere.
2. Ground-shock-induced airblast from contained explosions.[11, 12] Many applications, however, involve other than simple explosion geometries and are unsuited to calculational approaches. Where these geometries differ sufficiently, it is in order to make measurements to add to existing information.

One such opportunity existed in the March 9 detonation at the Old Reliable Mine near Mammoth, Arizona. There approximately four million pounds (2 kilotons) of ammonium nitrate were detonated to crush copper ore for in situ leaching. As described in detail later, the explosives were emplaced in horizontal side drifts ("coyote holes") perpendicular to horizontal main drifts mined into the ore body. The drifts were stemmed. Airblast could result from any of three causes, either singly or in combination: ground-shock-induced blast, blast from explosion gases breaking through the ground surface, and blast from stemming failure.

EXPLOSIVE EMPLACEMENT

The Old Reliable copper mine is located on the eastern edge of Pinal County, Arizona (Fig. 1). Figure 2 shows a cutaway perspective of the three levels. Figure 3 is the plan of each of the three levels, showing for each a main drift, coyote holes, charge emplacement, and stemming. Figure 4 shows the location of the three main drifts and their portals with respect to surface topography and the ore body. Commercial ammonium nitrate was the explosive. From the top down, the levels were referred to by the drift as the A level, 100-foot level, and 200-foot level. These levels were at MSL elevations of 3995, 3835, and 3735 feet respectively. The amount of explosive emplaced in the three levels was 596,000, 2,119,000 and 1,285,000 pounds respectively, for a total of 4,000,000 pounds. With the explosive in the A level detonated at zero time, the detonation of the 100- and 200-foot levels was planned for 105 and 200 msec, respectively. Actual detonation times were 89 and 144 msec.

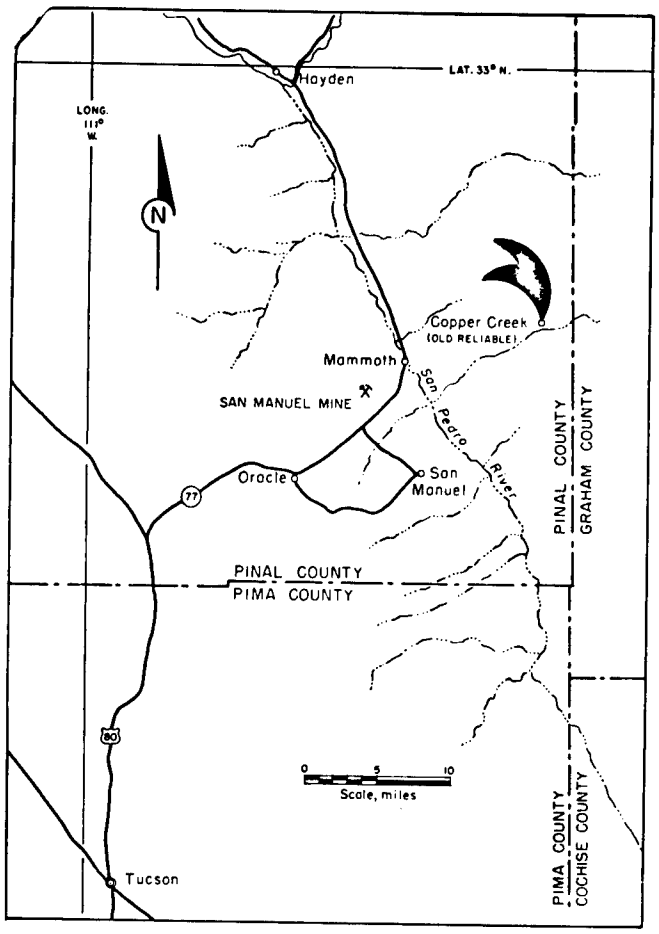

Figure 1. Location Map Showing Old Reliable Mine.

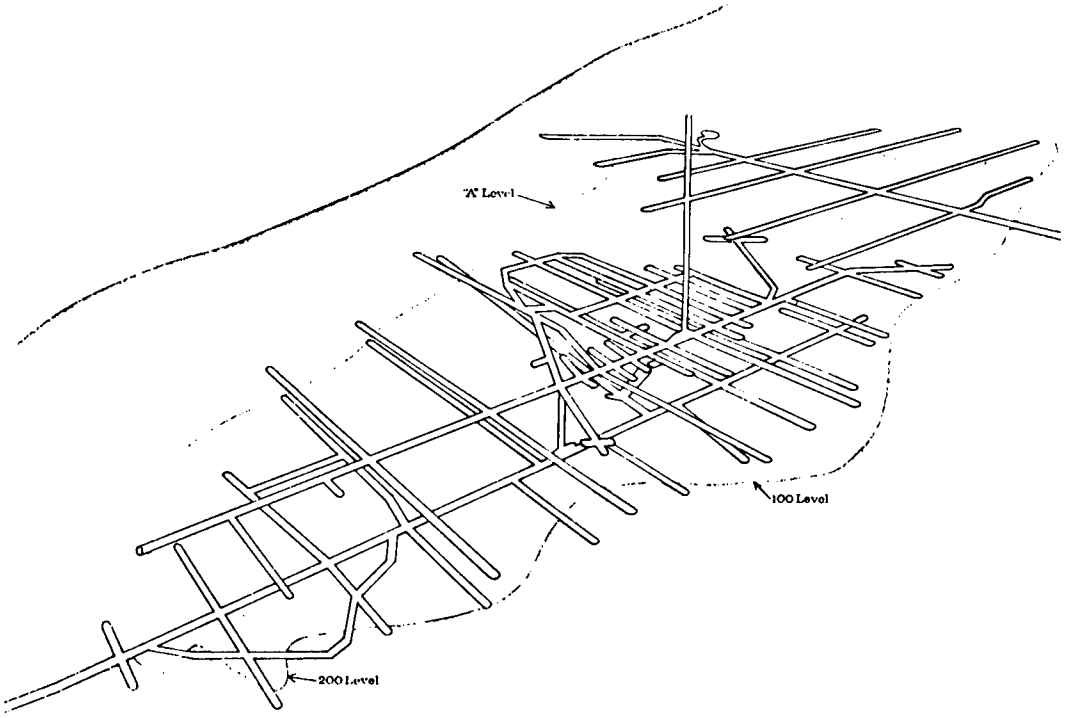

Figure 2. Tunnels and Crosscuts on Three Levels in Old Reliable Ore Deposit.

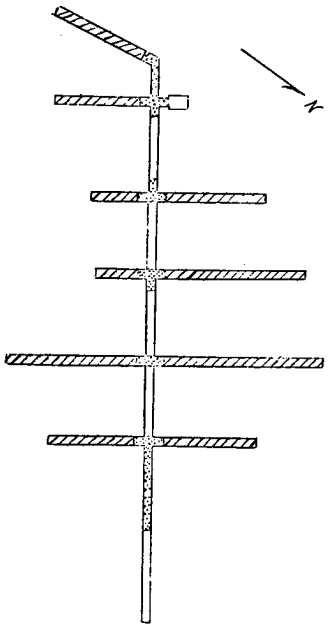

Scale: 100'

Explosives:

Stemming:

Old Reliable Blast - A Level

Emplacement of Charges & Stemming

Total Charge Weight on Level = 596,000 lbs.

Zero Delay

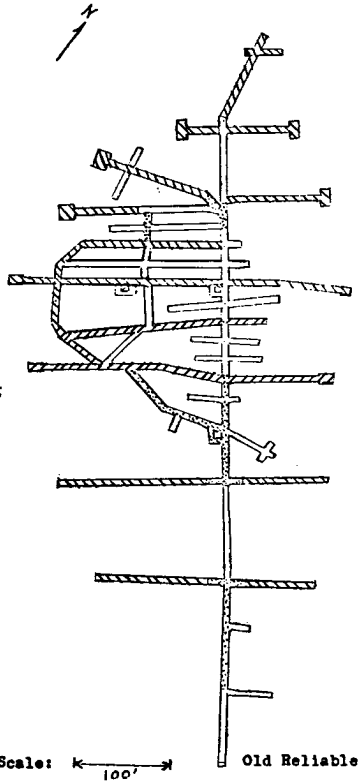

Scale: 100'

Explosives:

Stemming:

Old Reliable Blast - 100 Level

Emplacement of Charges & Stemming

Total Charge Weight on Level - 2,119,000 lbs.

89 ms Delay

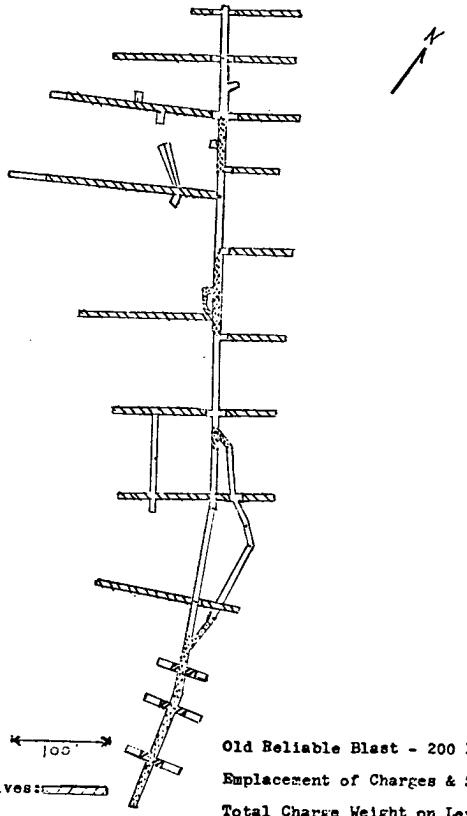

Scale: 100'

Explosives:

Stemming:

Old Reliable Blast - 200 Level

Emplacement of Charges & Stemming

Total Charge Weight on Level = 1,285,000 lbs.

144 ms Delay

Figure 3

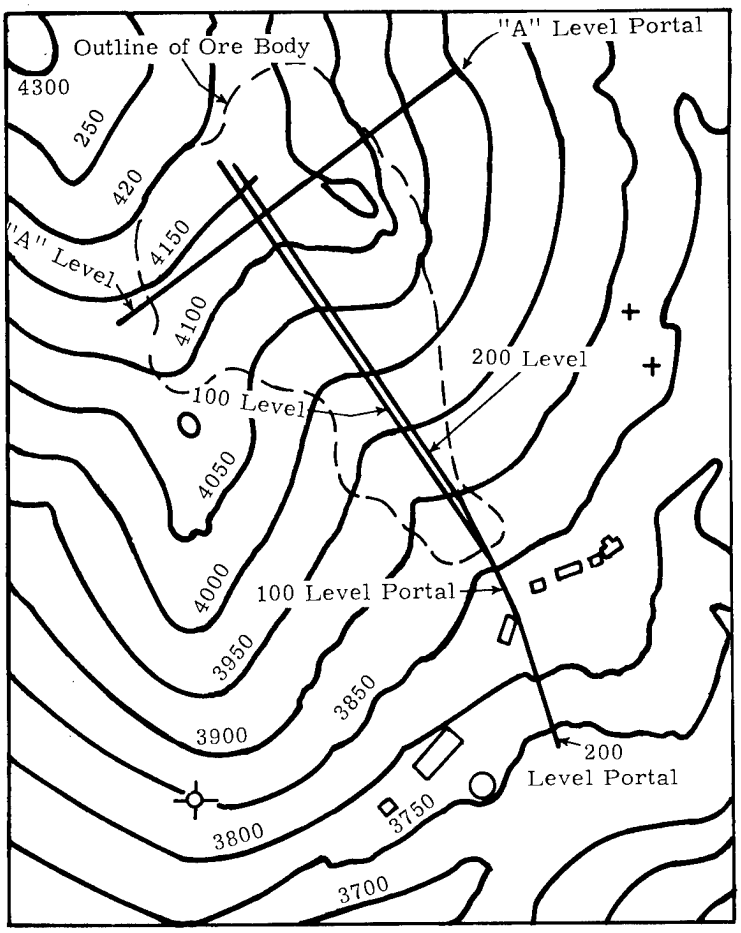

Figure 4. Location of Main Drifts and Portals with Respect to Topography and Ore Body.

OVERPRESSURE PREDICTIONS

The coyote holes were approximately 6 feet in diameter. Ammonium nitrate weighs approximately 56 lb/ft^3. Thus if the coyote holes were full, the explosive loading density would be 1583 lbs per linear foot of tunnel. At the time pre-shot estimates were made, the length of the coyote holes was not known and it appeared that the closest coyote hole to the sloping ground surface was at a slant distance of about 100 feet, or a scaled depth of 2.5 feet/(lb/ft$^{1/2}$). Spacing between coyote holes was also unknown, as was their location with respect to the surface, but since the main drifts tended to be perpendicular to the hill contours, each coyote hole after the outermost was assumed to be at a greater scaled depth of burial. Thus, if venting occurred other than through stemming failure, it would occur at the point of the shallowest coyote hole.

There is little or no information on airblast from buried line charges, which is what a single coyote hole constitutes. Measurements have been made, however, from row charges at a comparable scaled burial depth.[13] TNT charges weighing 64 lbs each, spaced 8 feet apart and buried 6 feet deep, had a scaled burial depth of 2.44 feet/(lb/ft$^{1/2}$). Measurements had been made on separate shots of 2, 5, 11, and 25 of these 64-lb charges. Results from the 5-charge row were chosen for comparison, since its line-charge equivalent length (40 feet and 14.1 feet/(lb/ft$^{1/2}$) would be comparable to a coyote hole 560 feet long -- a length greater than contemplated for the A-level in old reliable. Differences between ammonium nitrate and TNT were ignored. At a scaled distance of 35.4 feet/(lb/ft$^{1/2}$), the following overpressures were observed:

	Off end of Row	Perpendicular to Row
Ground-shock-induced peak (psi)	0.025	0.12
Gas-venting peak (psi)	0.055	0.10

Thus, maximum overpressure was observed perpendicular to the row and from ground shock.

For the mine shot, this value of 0.12 psi would occur at about 1400 feet (Point A in Fig. 5) from a single coyote hole 560 feet long. Peak overpressure would be increased by contributions from additional coyote holes at relatively greater scaled burial depths, but the amounts of these contributions would be difficult to estimate. If this pressure resulted from a point-source equivalent to a line 300 feet long (about the maximum length of coyote hole expected) and was cube-root scaled to the total 4 million pounds, the same pressure would appear at 2800 feet (Point B in Fig. 5).

One similar source of information from larger charges is Project Dugout.[14] There, five 20-ton nitromethane charges were buried 58.8 feet deep and 45 feet apart. This corresponds to a line charge of 890 lb per linear foot at a scaled depth of 1.97 feet/$(lb/ft)^{1/2}$. Maximum overpressure of 0.145 psi occurred at 1300 feet (Point C in Fig. 5) or, scaled to the 300-foot coyote hole considered above, at 2600 feet (Point D in Fig. 5).

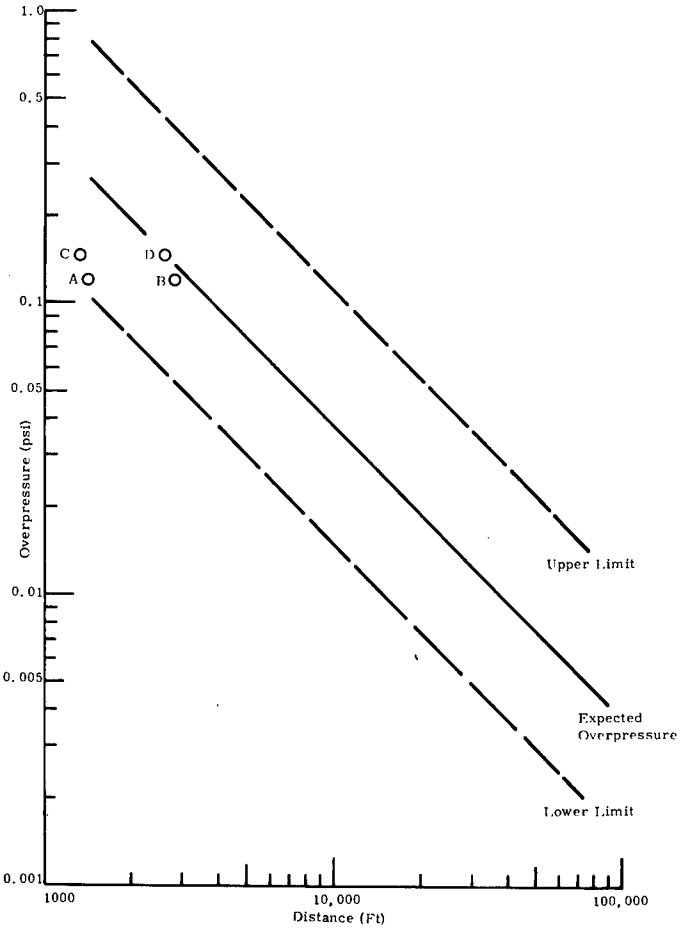

Figure 5. Peak Overpressure Predictions.

TABLE 1

SUMMARY OF AIRBLAST M

Station	Range (ft)		Time of Arrival (sec) (a)	Ground-Shock-Induced Peak Overpressure (psi)	Time of Peak (sec) (a)	End of Positive Phase (sec) (a)	Positive Impulse (psi-sec)	Peak Negative Pressure (psi)	T (P (
1	1610	LO	1.475	0.0277	2.285	2.715	0.0174	0.00974	4.
		HI	1.465	0.0264	2.300	2.715	0.0173	0.01370	4
2	3440	LO	2.615	0.0198	3.460	3.735	0.0115	0.00809	4
		HI	2.655	0.0182	3.460	3.750	0.0106	0.00850	5
3	6460	LO	5.245	0.0101	6.090	6.440	0.0060	0.00490	7
		HI	5.295	0.0102	6.135	6.450	0.0055	0.00467	7
4	13670	LO	11.605	0.00422	12.525	12.875	0.00258	0.00206	14
		HI	11.790	0.00447	12.485	12.885	0.00258	0.00202	14
5	24740 (24910)(b)	LO(c)	21.685	0.00101	22.475	22.870	0.00064	0.000477	24
		HI(c)	21.670	0.00178	22.440	22.865	0.00111	0.000880	24
6	48800 (50200)(b)	LO	44.275	0.00135	44.900	45.135	0.00071	0.000682	45
		HI	44.280	0.00127	44.915	45.120	0.00073	0.000685	45
7	61000	LO	53.525	0.000765	54.205	54.720	0.00047	0.000435	56
		HI	53.565	0.000801	54.205	54.715	0.00048	0.000481	56

(a) All times are based on an arbitrary zero time. Times to true zero (estimated) can be obtained by adding 0.410 seco

(b) Location based on arrival time.

(c) All amplitudes are low for unknown reason.

(1)

TABLE 1

SUMMARY OF AIRBLAST MEASUREMENTS

Peak Negative Pressure (psi)	Time of Peak (sec) (a)	End of Negative Phase (sec) (a)	Negative Impulse (psi-sec)	Peak Reflection Overpressure (psi)	Time of Peak (sec) (a)	End of Reflection Pulse (sec) (a)	Reflection Pulse Impulse (psi-sec)	Energy Flux (psi^2-sec)
0.00974	4.360	6.850	0.0261	0.01480	7.495	8.530	0.0101	0.000555
0.01370	4.000	6.870	0.0256	0.01770	7.495	8.210	0.0113	0.000580
0.00809	4.940	8.040	0.0165	0.00887	8.490	9.265	0.0054	0.000263
0.00850	5.205	8.045	0.0171	0.00913	8.665	9.220	0.0047	0.000252
0.00490	7.910	10.755	0.00935	0.00501	11.250	11.790	0.00275	0.0000727
0.00467	7.930	10.740	0.0093	0.00461	11.195	11.765	0.00250	0.0000655
0.00206	14.220	17.175	0.00448	0.00236	17.615	18.230	0.00133	0.0000142
0.00202	14.385	17.220	0.00448	0.00236	17.595	18.240	0.00133	0.0000143
0.000477	24.245	27.115	0.00095	0.00474	27.580	28.105	0.00013	-
0.000880	24.255	27.120	0.00172	0.000788	27.540	28.115	0.00042	0.0000024
0.000682	45.415	49.560	0.00107	0.000592	50.005	50.475	0.00027	0.00000106
0.000685	45.465	49.645	0.00109	0.000601	50.000	50.605	0.00023	0.00000113
0.000435	56.135	57.860	0.00073	0.000367	59.545	60.185	0.00040	0.000000583
0.000481	56.080	57.875	0.00073	0.000388	59.815	60.150	0.00041	0.000000573

.ined by adding 0.410 seconds to all times shown.

SUREMENTS

ıe k c)	End of Negative Phase (sec)	Negative Impulse (psi-sec)	Peak Reflection Overpressure (psi)	Time of Peak (sec)	End of Reflection Pulse (sec)	Reflection Pulse Impulse (psi-sec)	Energy Flux (psi^2-sec)	Energy $\frac{in\text{-}lb}{10^5}$
.)	(a)			(a)	(a)			
360	6.850	0.0261	0.01480	7.495	8.530	0.0101	0.000555	18480
300	6.870	0.0256	0.01770	7.495	8.210	0.0113	0.000580	19310
340	8.040	0.0165	0.00887	8.490	9.265	0.0054	0.000263	22730
05	8.045	0.0171	0.00913	8.665	9.220	0.0047	0.000252	21780
10	10.755	0.00935	0.00501	11.250	11.790	0.00275	0.0000727	22160
30	10.740	0.0093	0.00461	11.195	11.765	0.00250	0.0000655	19960
20	17.175	0.00448	0.00236	17.615	18.230	0.00133	0.0000142	19380
85	17.220	0.00448	0.00236	17.595	18.240	0.00133	0.0000143	19520
45	27.115	0.00095	0.00474	27.580	28.105	0.00013	-	-
55	27.120	0.00172	0.000788	27.540	28.115	0.00042	0.0000024	10730
15	49.560	0.00107	0.000592	50.005	50.475	0.00027	0.00000106	19510
65	49.645	0.00109	0.000601	50.000	50.605	0.00023	0.00000113	20800
35	57.860	0.00073	0.000367	59.545	60.185	0.00040	0.000000583	15830
80	57.875	0.00073	0.000388	59.815	60.150	0.00041	0.000000573	15560

s to all times shown.

(3)

Assuming attenuation as 1/r, the line shown in Fig. 5 represents the expected peak overpressure. The high-range gage was set at about three times the expected overpressure and the low-range gage at 0.4 times the expected pressure. These set ranges allow adequate coverage for unexpectedly high overpressures such as might result from a stemming failure, or from higher or lower overpressures such as would result from inherent uncertainties. The set range is a guide such that exceeding the value by a factor of 1.5 to 2.5 will not cause excursion beyond the 10.5 percent telemetry band-edge.

INSTRUMENTATION

A blast line was chosen to run generally westward from the Old Reliable mine to the town of Mammoth in the San Pedro river valley. Six of seven station locations were chosen to be successive factors of 2 from the closest, which, at 1500 feet, was planned to be beyond the probable range of hits by ejected rocks. The seventh and most distant was located at the smelter town of San Manuel, to record blast incident on the town and to be near where seismic and structural-response measurements were to be made. The third station was shifted slightly from the blast line to accommodate the Sisters Ranch, where structural-response measurements were also to be made. The sixth was located in Mammoth, even though no other measurements were made there. Other stations were shifted to be near the Copper Canyon access road, to avoid unfavorable terrain features, or to coincide in some cases with bench marks, which made radial distances easily determinable without survey.

The pressure gages were Statham unbonded strain gages. Two gages differing in sensitivity were employed in a single canister. Signals were telemetered from the stations to an Ampex AR-200 recorder, installed in a van about 2 miles south of Mammoth on terrain that permitted good reception from all stations.

Records from the tapes were played back at Albuquerque and digitized at a rate of 200 hertz. Records presented herein, and all analyses, were done from digitized records.

A zero-time fiducial from the firing set was attempted, but a cable break apparently caused by rodents prevented transmission of the signal. An unsuccessful attempt was also made to record WWV.

RESULTS

The detonation occurred March 9, 1972, at 11:45 am, MST.

The original pressure/time records are reproduced in Appendix A, together with impulse time. Peak overpressures were approximately one-fifth those expected. As a result there were two unfavorable consequences where the measurements were concerned. First, and logically,

the low signal resulted in an undesirably low signal-to-noise ratio. Secondly, the low signal caused wind-induced transient changes in ambient pressure to have amplitudes that were appreciable percentages of signal amplitudes in some cases. The effects of these changes were especially apparent in integrations of pressure/time data (see Appendix A) when an interval of 50 seconds is considered.

The pressure signal spans an interval of 8 to 12 seconds and is clearly reproducible from one station to the next. The impulse/time curve preceding and following the signal was connected through the signal with an eyeball curve that in the author's judgment best represented the wind contributions. These curves were approximated by a series of straight lines and the wind effect deducted from the record. The results are shown in the records reproduced in Appendix B, where the records shown have also been sequentially smoothed digitally one to three times to reduce the noise level.

Table 1 summarizes the results of the pressure measurements portrayed in Appendix B.

The Explosion

Motion-picture coverage of the detonation identified the times of the following visible events:

1. Primacord detonation along the surface of the ground identified zero time.
2. A flash of flame at the 200-level portal occurred at 0.144 second and is probably associated with the 0.144-second delay.
3. Smoke jetted from the 200-level portal at 0.434 second, probably indicating a portal stemming failure.
4. Cracks opened in the surface above the A level, permitting dust and smoke to escape. The first of these occurred at 0.975 second, with others following quickly.
5. Plumes of rock were ejected and began impacting on the surface at 4 seconds or earlier and continued impacting until 6.1 seconds or later.
6. A major plume of smoke and gas escaped, with strong vertical jetting starting at 10.06 seconds and continuing for a considerable time.

It is these components that may be relatable to the shape of the blast wave.

Wave Shape

At all stations the wave shape was characterized by a positive pulse, a negative pulse, and a second positive pulse that peaked about 5.1 seconds after the first. The source of the second pulse is uncertain, but the following possibilities, in order of credibility, are offered.

a. The only mechanism visible in the motion pictures at a time that would coincide with the source of the signal is the "splash-down" of ejecta; for this reason it is listed as the most probable source.

b. The pulse could have been caused by a release of explosion gases (a gas-venting pulse) occurring simultaneously over a large surface area at very low velocity. The velocity would have to be low enough so that the motion it induced would not be visible through the dust cover, since no such action was evident in the motion pictures. The high-velocity plume seen later produced no measurable signal.

c. The explosions caused the ground surface to rise in an irregular mounding. The total height could not be determined because of dust obscuration, but the time of collapse is estimated to be approximately 3.3 seconds. Even if impact of collapsing material occurred later, generating a seismic signal, the mechanism by which impact could generate an airblast signal under these conditions is not clear. A squeezing out of residual cavity gas in the sense of item b above is one possibility.

d. The interval between the two pulses is relatively constant at all stations, indicating that the source is either at or near the epicenter, or beyond it along the axis of the blast line. If a reflection, the reflector would have to be located at a distance of about 2900 feet. In that direction is a hill beginning 200 feet horizontally from the 200-level portal and 300 feet from the A-level portal, rising 580 feet in 1100 feet from the 200-level portal and 1600 feet from the A-level portal. The hill would have returned a signal earlier because of its location and the signal would have been dispersed in time because of the slope.

e. The possibility of explosive afterburning of gases is not realistic for an oxygen-balanced explosive. There is no evidence in the photography of late detonations, and on available seismic records the effect of collapse of the mound would not be distinguishable from the effect of a late detonation.

The first positive pulse has a double peak, the first slightly smaller than the second. The peaks are separated by 190 to 440 msec (average 320 msec). This is longer than the interval between the first and third detonations, and the second peak probably reflects venting from the 200-level portal (Item 3 under the Explosion, above).

At the closest station there are signals preceding the positive pulse by 1.6 sec, which could be surface-wave induced. If so, the surface wave was traveling at 1920 ft/sec, based on the adjusted time described below.

Arrival Times

No zero-time signal was recorded, so the times of Table 1 are approximate. An estimate of zero time was made in the following way. Peak overpressures were quite small and signals would travel at essentially acoustic velocity.

No weather observations were made at shot time. Based on those at Tucson, the following ambient conditions are inferred:

Mammoth	86.1°F	930 mb
A-level	80.5°F	875 mb

These values indicate sonic velocities of 1140 ft/sec at the A-level elevation and 1146 ft/sec at Mammoth. The 1130 ft/sec velocity inferred below from transit times of pressure peaks corresponds to an ambient temperature of 70.7°F. The difference of 10 ft/sec is most likely attributable to an average up-slope wind velocity of 10 ft/sec (7 mph), which is within the range of subjective observations that winds were "light and variable" at the surface.

The peak of the positive pulse is a more accurately identifiable characteristic than the break-away from ambient pressure. If the times of peak shown in Table 1 are used, a propagation velocity of 1130 ft/sec is deduced for four of the seven stations, with an error in the nominal location of three stations indicated by the inconsistency with the other four. The peak should arrive at the 3440-foot station in 3.045 seconds, traveling at 1130 ft/sec. The peak follows the arrival at that station by an average of about 0.825 second, giving a true time for the peak of 3.870 seconds. This is 0.410 second more than the arbitrary time shown in Table 1. Therefore, 0.410 second should be added to times in Table 1.

In Table 1 the adjusted distance to the station, as derived from an average velocity of 1130 ft/sec, is shown in parentheses for the first, fifth, and sixth stations.

Positive Phase Duration

Duration of the positive phase of the ground-shock-induced pulse at the first five stations averaged 1179 msec. Duration of the ground-shock-induced pulse for single-charge explosions is shown in Table 2 for the deeper explosions. Duration is not especially sensitive to the deeper burial depths; it is more sensitive to medium. Compared with the pulse duration of the Buckboard shot, the Old Reliable detonation duration is equivalent to that of a 2.4-million-pound single TNT explosion.

TABLE 2

Duration of Ground-Shock-Induced Pulses

Event	Scaled DOB $ft/lb^{1/3}$	Duration msec	Scaled Duration $msec/lb^{1/3}$	Medium
Stagecoach 3	2.3	152	4.44	NTS/Alluvium
CAPSA 6	1.75	44.4	4.44	ABQ/Alluvium
CAPSA 11	1.5	140	4.48	ABQ/Alluvium
Buckboard 13	1.75	140	4.09	Basalt

Peak Overpressure

Figure 6 shows the peak overpressure of the first pulse plotted against distance. Peak overpressure attenuates with distance about as r^{-1}. At the 24,740 station, the amplitudes are 68 and 39 percent (for high and low range respectively) of those indicated by other stations. Records were carefully checked for calibration error and none was found. The fact that the low-range gage was affected more than the high-range gage indicates an effect involving the gage intake port, but no mechanism is obvious.

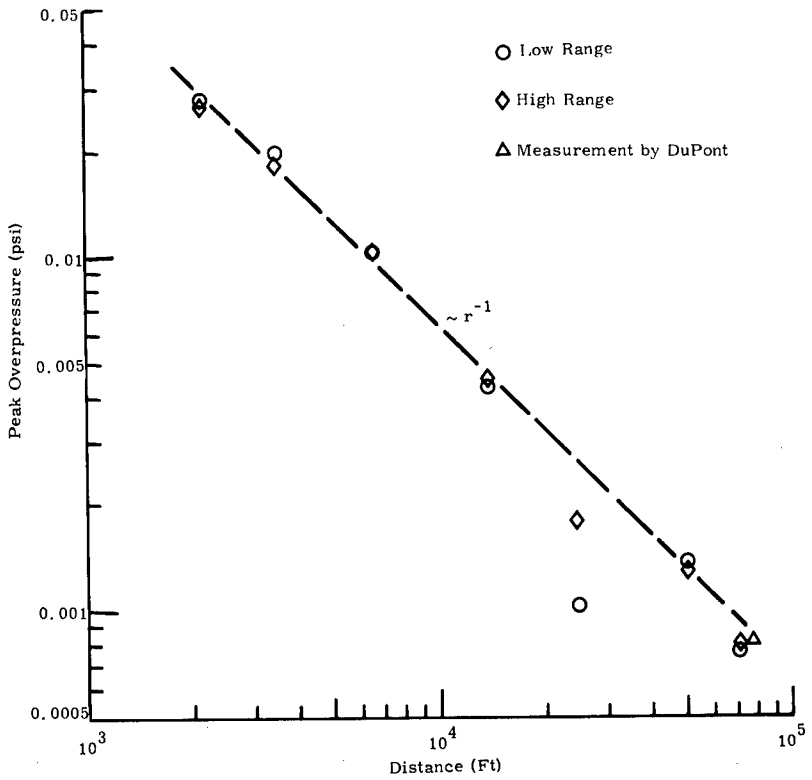

Figure 6. Measured Peak Overpressures.

Pressure at the San Manuel station (61, 000) is slightly low, but this can be attributed to the fact that its transmission path at an azimuth of 220° was different from the path of the balance of the blast line at about 260°. Also, the measurement agrees with one made by DuPont a mile farther away.

Peak overpressures were only about 1/6 those expected. Clearly, dispersing the charge in side drifts greatly reduces the ground shock that originates the pressure pulse, resulting in overpressures less than predicted. Delayed detonation of the 100- and 200-levels adds their contributions to the peak overpressure and pulse duration generated by the detonation of the A level.

Since the purpose of making the measurements is to relate the airblast from a dispersed configuration to airblast from single-charge, row-charge, and line-charge detonations within accumulated experience, the following paragraphs are devoted to exploring relationships that could not be explored with the limited information available pre-shot.

The approach used in the comparison employs the airblast measured on past explosions of buried rows and quincuncial arrays of charges, and consists of the following steps:

a. The charges in all coyote holes for a given level are summed into an equivalent continuous single-line charge considered to be under level terrain at the average burial depth $\overline{(dob)}$ of all the coyote holes.

b. The line charge is converted to an equivalent row of charges evenly spaced about 0.8 times $\overline{dob}$. Spacing and charge size are adjusted to the nearest whole charge.

c. One charge in the row is treated as a single charge and its peak overpressure determined from relationships derived from a large number of measurements.

d. The peak overpressure of this "single" charge is multiplied by a factor related to the number of charges in the row. The factor was derived from measurements of airblast from row-charge shots of from 1 to 25 charges. For the quincuncial arrays the procedure is similar, involving the following steps:

a. Same as above.

b. The line charge is converted to an equivalent quincuncial array at $\overline{dob}$.

c. The surface area significantly affected by ground shock is estimated, and the charge density per unit area is determined.

d. The spacing of a quincuncial array of 64-lb charges with the same charge density per unit area is determined, assuming the area within the boundary of the array is effective in producing ground-shock-induced airblast.

e. The 64-lb charge array airblast measurements are used as a basis for the estimates and are scaled to the larger shot using cube-root scaling.

Figure 3 shows that the A-level contained 596,000 pounds of explosive in approximately 1025 feet of drift. Loading density averaged about 580 lb/ft. The charge had a weighted average vertical burial depth of 143 feet. This was obtained from $\frac{\Sigma \ell \bar{d}}{L}$, where ℓ is the length of an individual drift, $\bar{d}$ is the average depth over the length of a given side drift, and L is the total length of a side drift. Slant burial depth averages 127 feet beneath the 27° slope. The line-charge scaled burial depth was $127/580^{1/2}$ or $5.27\ \text{ft/(lb/ft)}^{1/2}$. This is considerably deeper than indicated by pre-shot predictions, both because the amount of cover over the drifts was greater and because the loading density of the explosive was less than anticipated.

Work with row charges has shown[15] that a row-charge is equivalent to a line charge from a cratering standpoint if the scaled spacing |(s)| is not greater than 0.8±0.2 dob, dob is the scaled burial depth, and both s and dob are in $\text{ft/lb}^{1/3}$. If the same equivalence applies for airblast, the loading of the A level would correspond to a row of ten 59,600-lb charges spaced 103 feet apart (59,600 lb ÷ 580 lb/ft) and buried 127 feet deep. The single-charge scaled burial depth would be $3.25\ \text{ft/lb}^{1/3}$.

Ground-shock-induced peak overpressure from single charges detonated in hard rock (basalt) at scaled depths between 0.75 and 1.75 was found[5] to follow the relationship

$$\Delta p = \frac{3.5\left(\frac{r}{W^{1/3}}\right)^{-1.03}}{10\ \exp\left(0.47\ \frac{dob}{W^{1/3}}\right)} \qquad (1)$$

This was based on measurements made only to a scaled distance of $10\ \text{ft/lb}^{1/3}$. If the relationship is assumed to apply at greater burial depths and ranges, a single 59,600-lb charge at 127 feet would produce a peak overpressure of 0.00034 psi.

An experiment with row charges at both shallower burial depth and closer spacing showed that the dependence of ground-shock-induced peak overpressure on number of charges in the tow was n^{α} where α was from 0.8 to 0.95 for the combination of spacings and burial depths examined. Again, assuming that the relation holds for other spacings and burial depths, and using an average value for α, gives a peak overpressure of 0.0025 psi at 10,000 feet for the ten-charge row corresponding to the A-level detonation. This is 40 percent of the peak measured at that distance, indicating either that the estimating procedure just described is inadequate or that the contribution of the 100- and 200- levels was considerable. Both possibilities will be examined.

Airblast measurements have been made on a horizontal square array of 5 small charges.[16] Simply because this constitutes another set of data to be compared with airblast from the dispersed charge, a comparison will be sought. Scaled burial depths reached $2.5\ \text{ft/lb}^{1/3}$, based on

individual charge weight. The ground surface area that produces ground-shock-induced airblast changes as charge spacing is changed.

The A-level detonation was also a dispersed-charge explosion. The dimension of the charge array was roughly 500 feet long by an average of 200 feet wide. Let it be assumed that the airblast was generated by this ground surface area. The dispersed charge would be equivalent to a 5-charge array of 119,200-lb charges at a slant depth of 127 feet (2.6 ft/lb$^{1/3}$), and spaced in a 316-foot square. The scaled depth is close to the deepest small-charge shots and the spacing would correspond to five 64-pound charges in a 7.3-foot square. This gives similarity in charge density; i.e., 5.96 lb/ft^2. Measurements 500 feet (125 ft/lb$^{1/3}$) from the 64-pound charge array with 10 and 16-foot spacings, indicate that pressure extrapolated to the 7.3-foot spacing would be about 0.007 psi. Extending this to a scaled depth of 2.6 ft/lb$^{1/3}$ by the relationship of Eq. 1 reduces the overpressure to 0.0063, and extending this to a scaled distance of 203 ft/lb$^{1/3}$ (10,000 feet from the A-level detonation) by r^{-1} further reduces the peak overpressure to 0.0039 psi. This is 60 percent of the measured pressure at that distance and 1-1/2 times the value estimated on the basis of row charges. The small-charge measurements were made from detonations in soil rather than rock, so 0.0039 psi is probably a low estimate for comparison with the Old Reliable detonation.

The two estimates using rows and arrays of charges equivalent to those on the A-level, yield values about 40 to 60 percent of those measured. Thus, it remains to examine the contribution from the other two levels.

The 100 level had 2.119 million pounds of explosive in 2245 feet of drift: an average loading density of 944 ft/lb. The weighted average vertical burial depth was 248 feet; slant burial depth was 221 feet. The line-charge equivalent scaled burial depth was 7.2 ft/(lb/ft$^{1/2}$). The explosive in this level corresponds to a row of thirteen 163,000-lb charges spaced 173 feet apart. Using Eq. 1 again for peak ground-shock-induced overpressure from a single 163,000-lb charge at 10,000 feet results in a peak of 0.000205 psi. For a thirteen-charge row this becomes 0.00195 psi at 10,000 feet.

The 200 level had 1.285 million pounds of explosive in 1505 feet of drift for an average loading density of 854 lb/ft. The weighted vertical average burial depth is 283 feet; slant burial depth was 252 feet $\left(8.6 \text{ ft/(lb/ft}^{1/2})\right)$. This corresponds to a row of eight 160,600-lb charges spaced 188 feet apart. Equation 1 gives a peak overpressure at 10,000 feet from a single charge of 0.000108 psi. An 8-charge row would increase the overpressure to 0.00066 psi.

The sum of the contributions of the three levels is 0.0051, approximately 80 percent of the measured value at 10,000 feet.

The 5-charge-array analogy has not been applied to the 100 and 200 levels because the greater depths require extrapolation far beyond the range of parameters in the small-scale experiment. Had the analogy been used, however, the result would have yielded pressures higher than 75 percent of those measured.

If the three detonations had been simultaneous and at the same scaled burial depth, adding the peaks from each would be appropriate. The difference in depth would cause a small separation in time between peaks, and the delays would extend it further. The ground shock from the second and third detonations passes through rock disturbed by the first, and shock transmission therefore may be degraded. The above estimates were made on the assumption of undisturbed rock, and peak overpressure is likely overestimated.

An assumption of a simultaneous detonation of 4 million pounds of explosive at a weighted slant burst depth of 211 feet at an average density of 838 lb/ft in 4775 feet of drift, and using the row-charge analogy, gives a peak overpressure less than that obtained by adding the contributions of the separate levels.

Treating the explosion as a single 4-million-pound charge at the weighted average slant burial depth of 211 feet, and using Eq. 1, gives 0.0116 psi, or nearly twice that measured. Treating the charge at each of the three levels as single charges and summing their contributions results in a prediction more than twice that measured.

If, however, the entire explosion is considered as from a single 2.4-million-pound charge, as was derived from the positive-phase duration, Eq. 1 gives a peak overpressure only 20 percent greater than that measured. Since the positive-phase duration cannot be known in advance, this procedure is not available for prediction. Rather it indicates an internal consistency in ground-shock-induced airblast phenomena.

Measured pressures fall about midway between those of a prediction based on the sum of pressures contributed by three equivalent row charges, and one in which all the explosive was treated as a single charge.

Positive Impulse

Positive impulse was attenuated with distance as r^{-1} (Fig.7). Departures at the fifth and seventh stations were for the same reasons as in the case of peak overpressure. Reference 5 gives the following expression for positive-phase impulse from detonations in basalt:

$$I = \frac{11\left(\frac{r}{W^{1/3}}\right)^{-0.12}}{10\exp\left[0.54\left(\frac{r}{W^{1/3}}\right)^{0.28}\left(\frac{dob}{W^{1/3}}\right)\right]} \quad \text{(a)}$$

The expression breaks down for the application here because the waveforms of those shots contained a gas-venting pulse that is missing from the waveforms of this explosion.

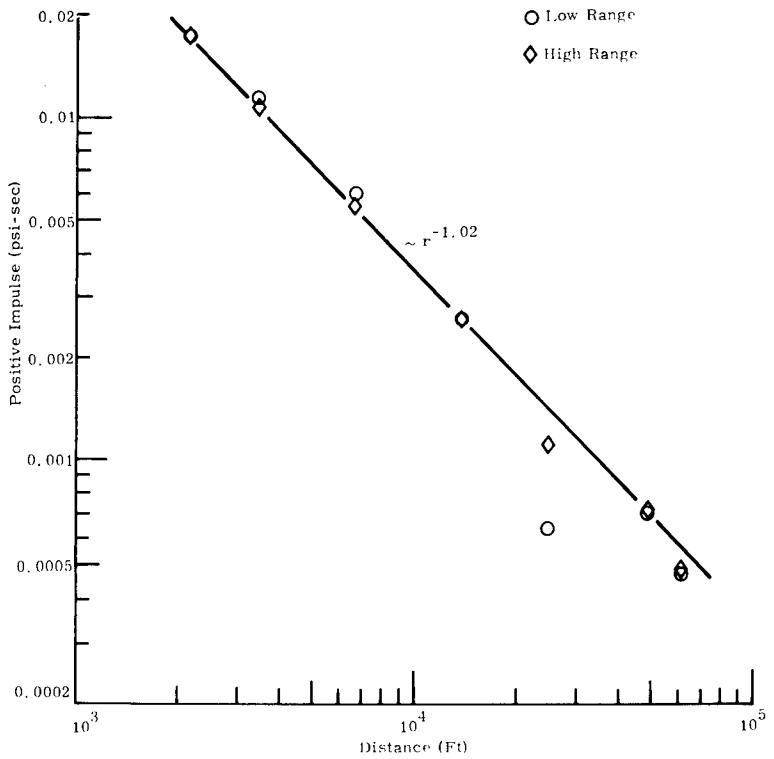

Figure 7. Measured Positive Phase Impulse.

Plots are not presented for peak negative pressure, negative phase impulse, or second peak pressure. The negative parameters attenuated with distance as $r^{-0.94}$ while the second-peak pressure attenuated as $r^{-1.02}$.

Airblast Energy

Appendix B contains plots of energy-flux-time, presented for possible further analyses. Only two observations are made at this time. If it is assumed that energy density is uniform over a hemisphere with a radius equal to the distance to the gage station, the total energy contained in the airblast wave (to the end of the negative phase) is listed in the last column of Table 1. The energy is essentially constant with distance, as it would be if the airblast envelope was a hemisphere with uniform energy density, indicating that the assumption is reasonable. If energy had increased with distance, it would have indicated a hemisphere with greater density at higher vertical angles feeding tangentially downward to the ground-level gages. It would appear that whatever energy gradients may have existed were too weak for tangentially downward equalization over the distances involved. The energy values of the last column of Table 1 are about equivalent to those from a 1000-pound surface-burst TNT explosion. This attests to the efficiency of reducing airblast by burial and dispersion of the charge.

CONCLUSIONS

Measurements of airblast from the detonations of ammonium nitrate at the Old Reliable mine gave waveforms consisting of a ground-shock-induced positive pulse, a negative phase, and a second positive pulse from an unidentified source. An attempt was made to correlate measured peak overpressures with those from equivalent single-charge, row-charge, and horizontal-array-charge detonations. The results indicate that retrospective predictions for this complex explosive configuration based on equivalent row charges were 20 percent less than measured values. Other correlations attempted gave less agreement.

REFERENCES

1. Effects of Impact and Explosion, Vol. I, Summary Technical Report of Division 2, NDRC, Department of Defense, Washington, D. C., 1946.

2. The Effects of Nuclear Weapons, S. Glasstone, editor, Rev. Ed., DOD/AEC, U. S. Gov't Printing Office, Washington, D. C., April 1962.

3. Vortman, L. J., "Air-Blast Suppression as a Function of Explosive-Charge Burial Depth," J. Acoust. Soc. of Amer., Vol. 40, No. 1, July 1966.

4. Vortman, L. J. Air-Blast from Underground Explosions as a Function of Charge Burial, Proceedings of Conference on Prevention and Protection Against Accidental Explosion of Munitions, Fuels, and Other Hazardous Materials (10-13 October 1966), Annals of the New York Academy of Sciences, October 28, 1968.

5. Vortman, L. J., "Close-in Airblast From Underground Detonations" in Proceedings of Symposium on Engineering with Nuclear Explosives, January 14-16, 1970, The American Nuclear Society and the U. S. Atomic Energy Commission, May 1970, pp. 1508-1543.

6. Kirkwood, J. G., and Brinkley, S. R., Jr., Theoretical Blast-Wave Curves for Cast TNT, OSRD-5481, NDRC A-341, Office of Scientific Research and Development, August 23, 1945.

7. Bethe, H., et al., Blast Wave, LA-2000, Los Alamos Scientific Laboratory, Los Alamos, New Mexico, March 27, 1958.

8. Broyles, C. D., IBM Problem M Curves, SC-TM-268-56(51), Sandia Corporation, December 1, 1956.

9. Whitaker, W. A., Air Force Weapons Laboratory, Personal Communication.

10. Lehto, D. L. and R. A. Larson, Long Range Propagation of Spherical Shockwaves from Explosions in Air, NOLTR 69-88, U. S. Naval Ordnance Laboratory, Explosions Research Department, White Oak, Maryland, July 1969.

11. Montan, D. N., "Source of Airblast from the Underground Explosion," Transactions, American Nuclear Society, Vol. II, No. 2, November 1968, pp. 541-542.

12. Cole, R. K. Jr., Acoustic Calculation of Ground-Shock-Induced Air Blast, SC-RR-70-734, Sandia Laboratories, Albuquerque, New Mexico, November 1970.

13. Vortman, L. J., Airblast and Craters from Rows of Two to Twenty-five Charges, SC-RR-68-655, Sandia Laboratories, Albuquerque, New Mexico, January 1969.

14. Vortman, L. J., Close-in Airblast from a Row Charge in Basalt, PNE-608F, Sandia Corporation, Albuquerque, New Mexico, August 1965.

15. Vortman, L. J., and Schofield, L. N., The Effect of Row Charge Spacing and Depth on Crater Dimensions, SC-4730(RR), TID-4500, Sandia Corporation, Albuquerque, New Mexico, November 1963

16. Rappleyea, C. Annette, Crater, Ejecta, and Air-Blast Studies From Five High-Explosive Charges in a Horizontal Square Array, SC-RR-66-480 TID 4500, Sandia Corporation, Albuquerque, New Mexico, April 1967.

APPENDIX A

Plots of Pressure-Time and Impulse-Time as Measured

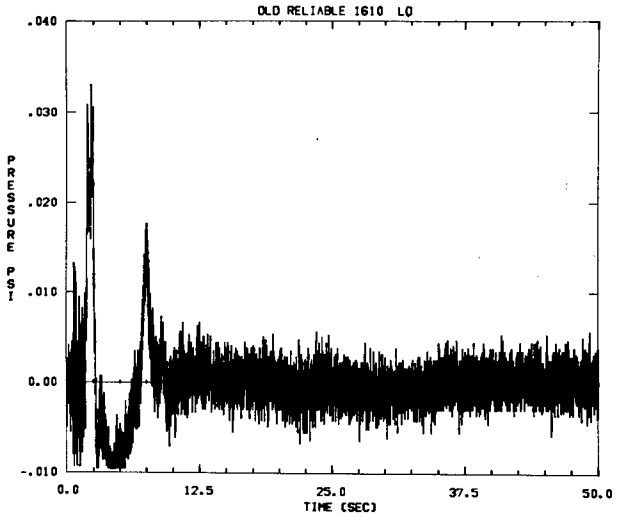

A= -.00467261

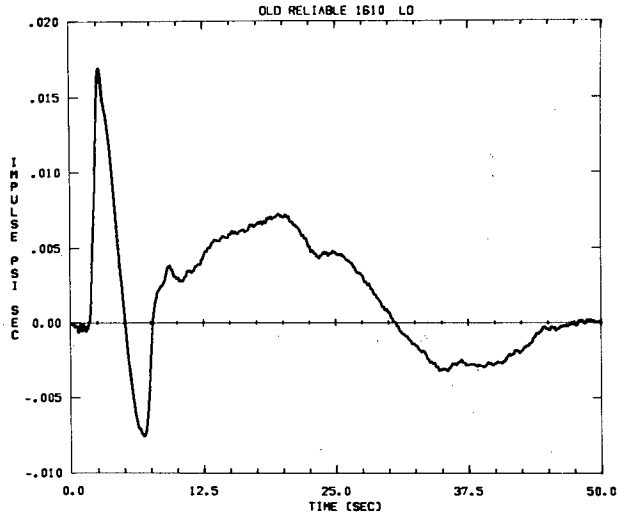

A= -.00467261

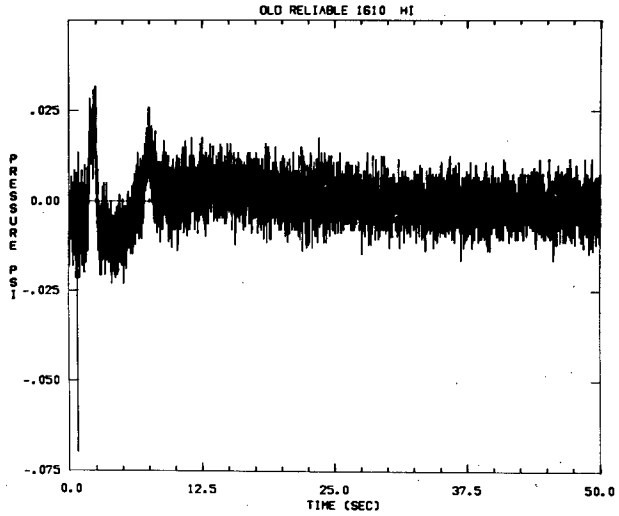

A= -.0210678

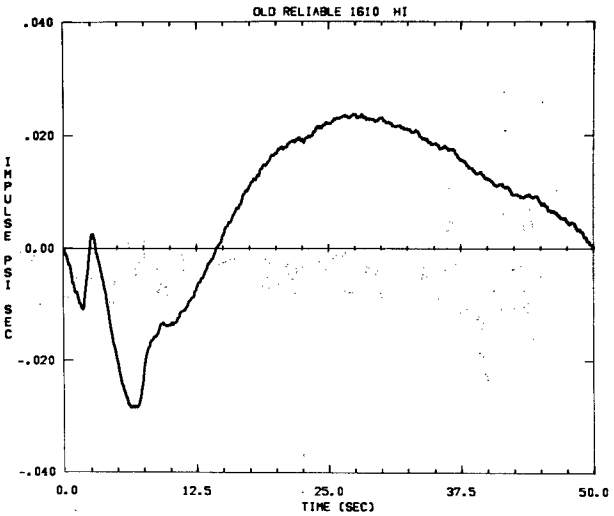

A= -.0210678

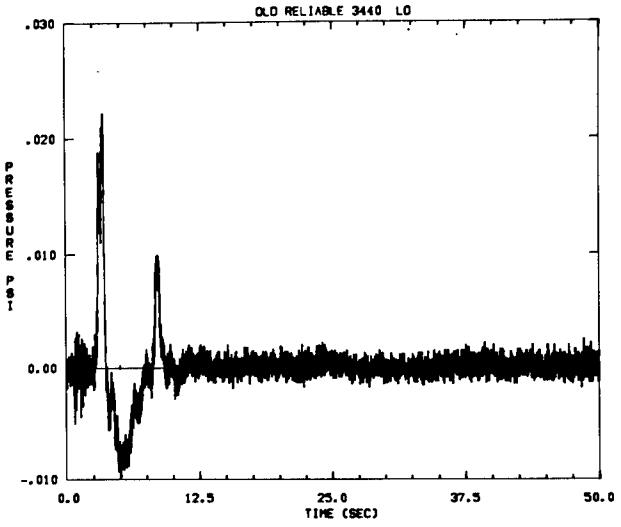

A= -.00070726

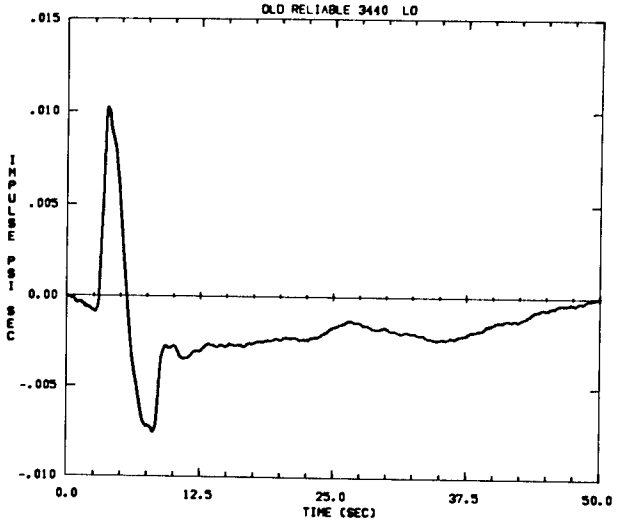

A= -.00070726

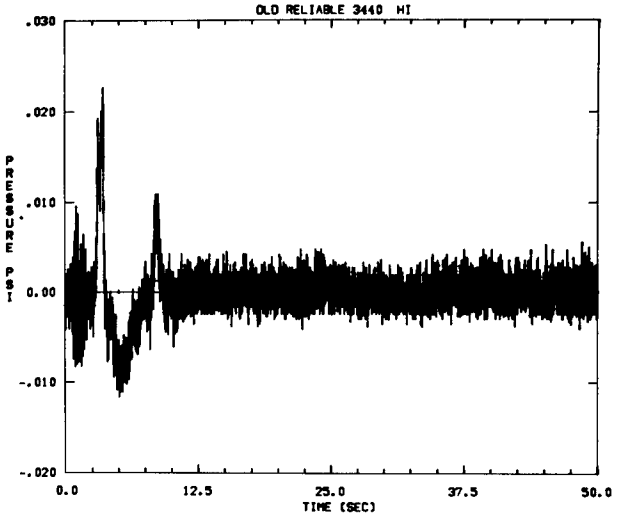

A= -.00312608

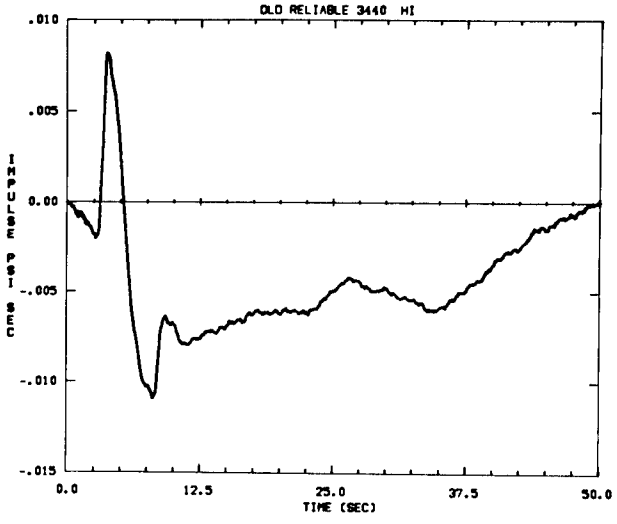

A= -.00312608

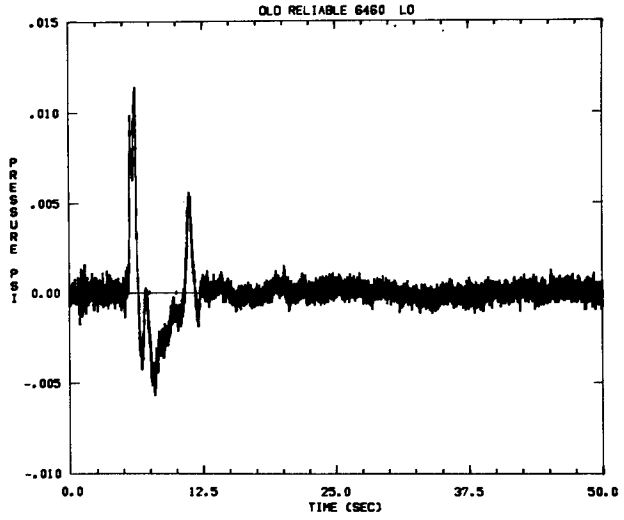

A= .00159349

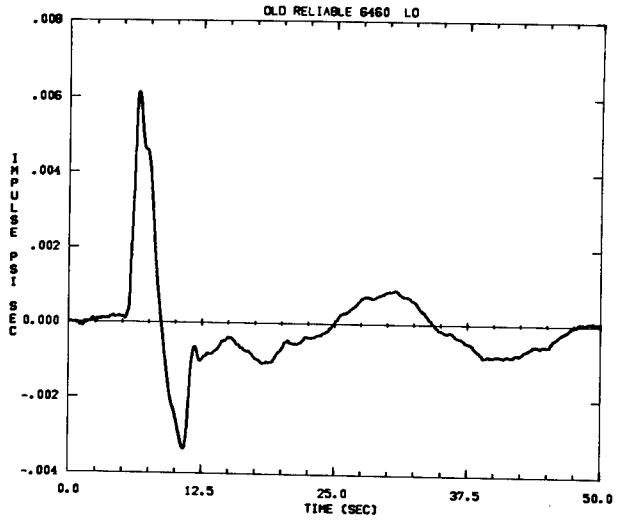

A= .00159349

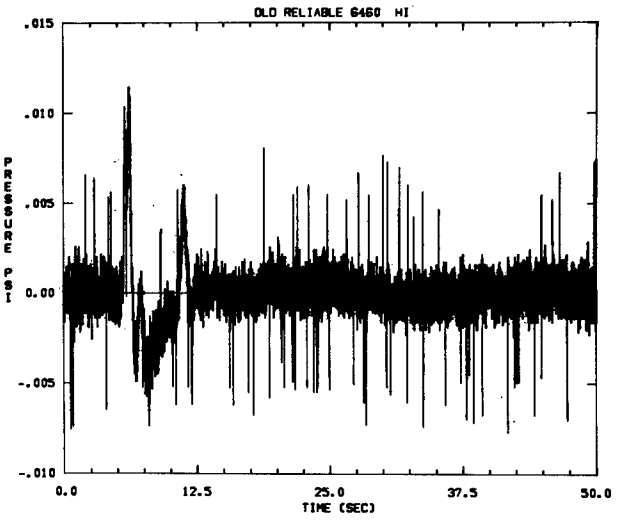

A= -.0159154

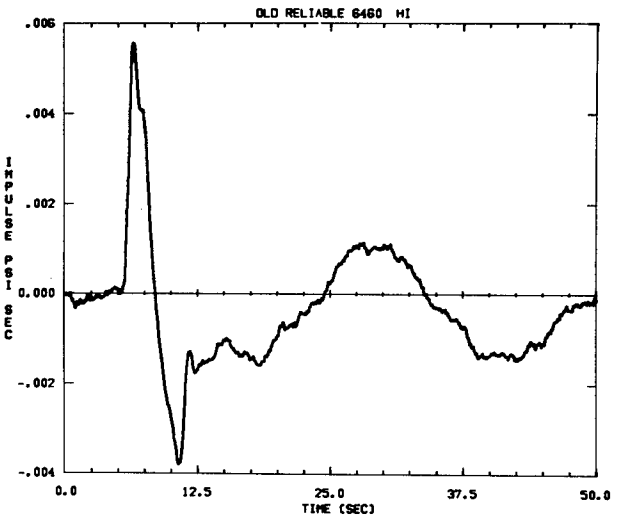

A= -.0159154

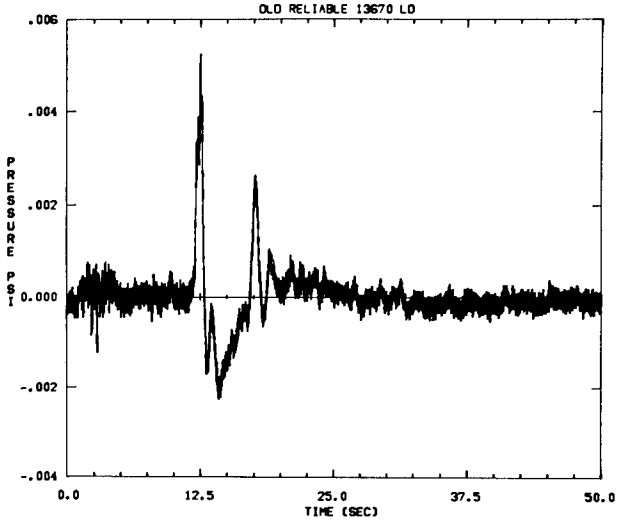

A= -.00050043

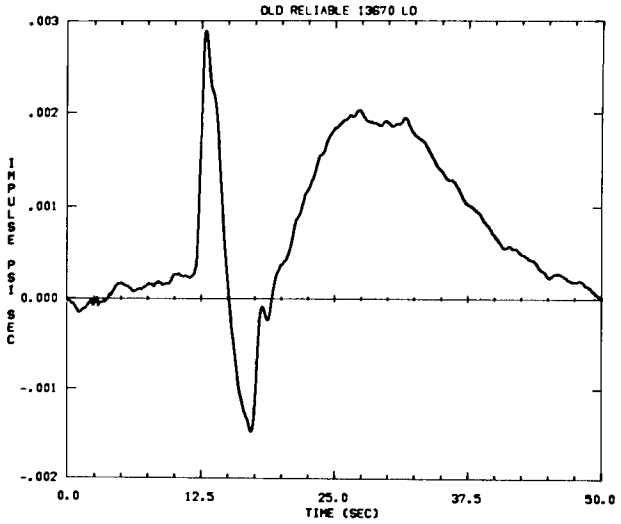

A= -.00050043

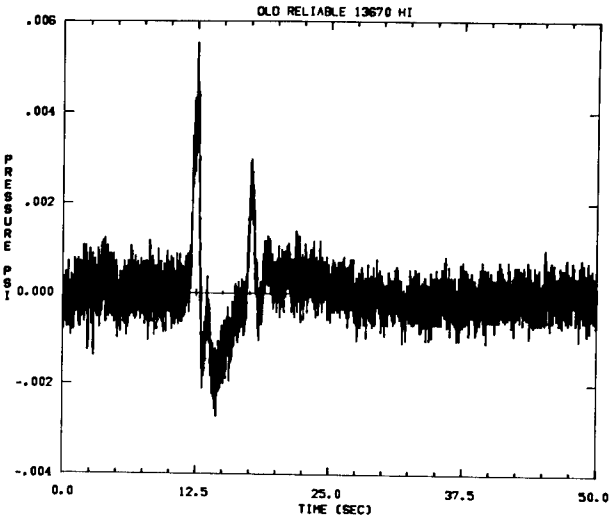

A= -.00086527

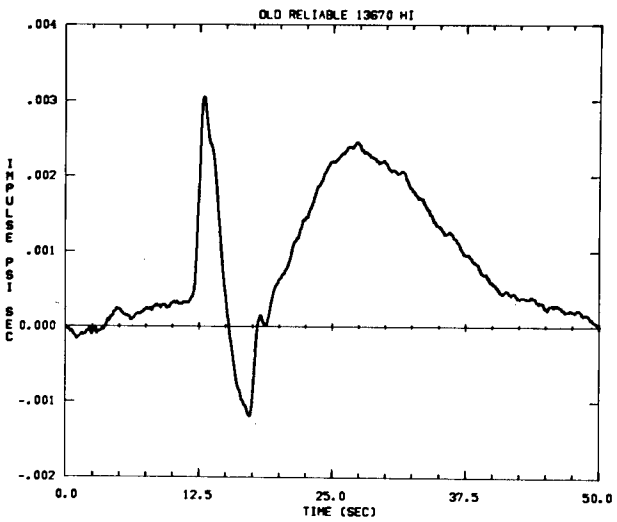

A= -.00086527

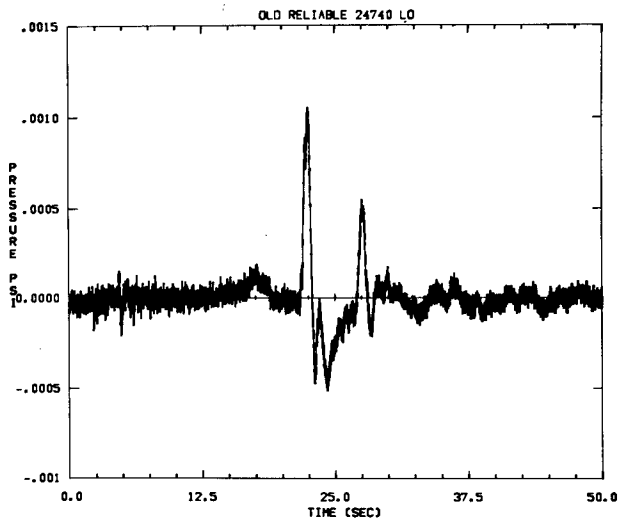

A= -.00547245

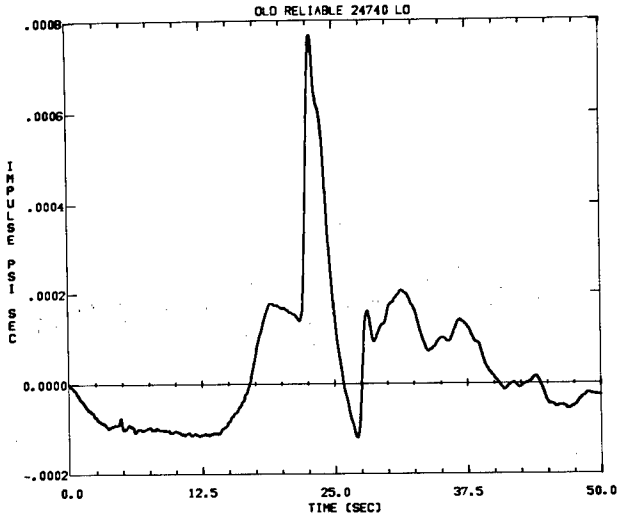

A= -.00547245

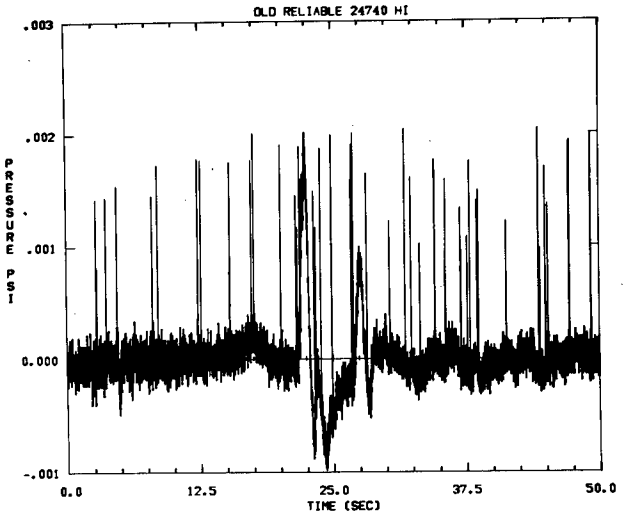

A= .0156329

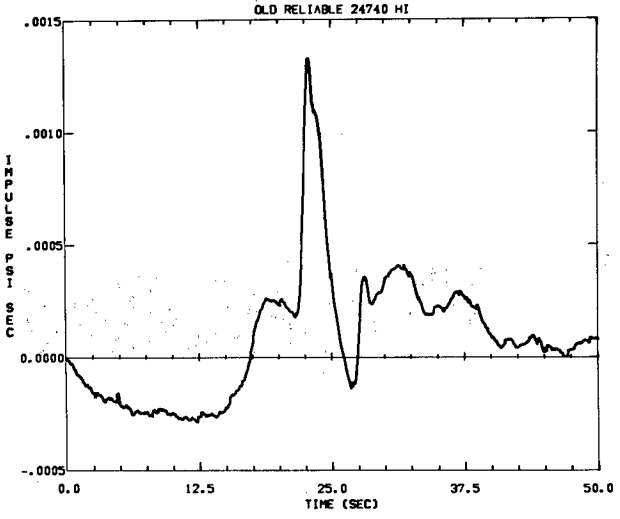

A= .0156329

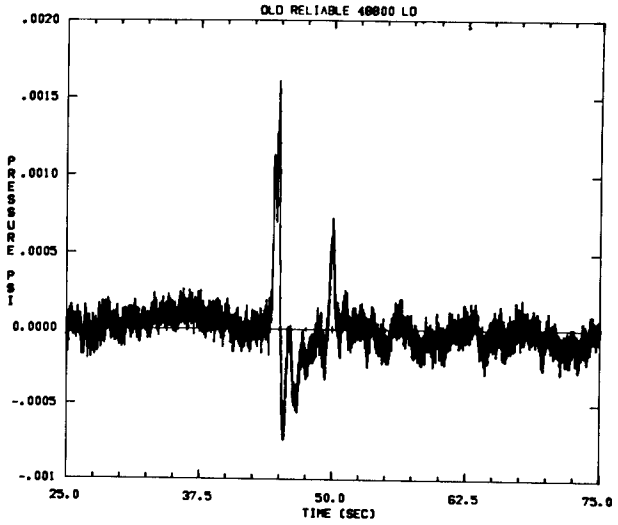

A= -.00073000

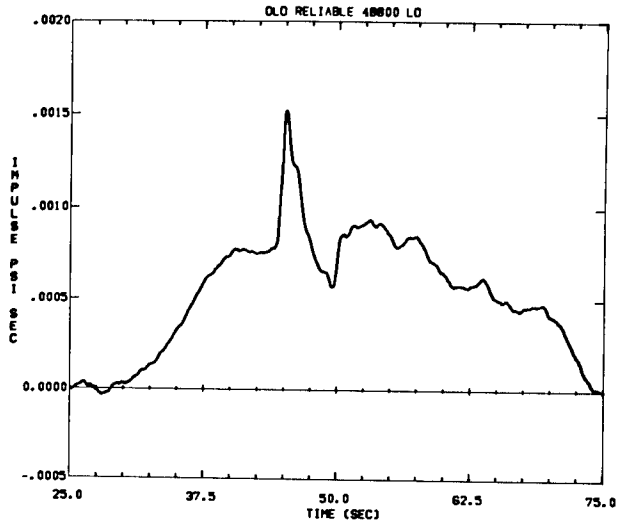

A= -.00073000

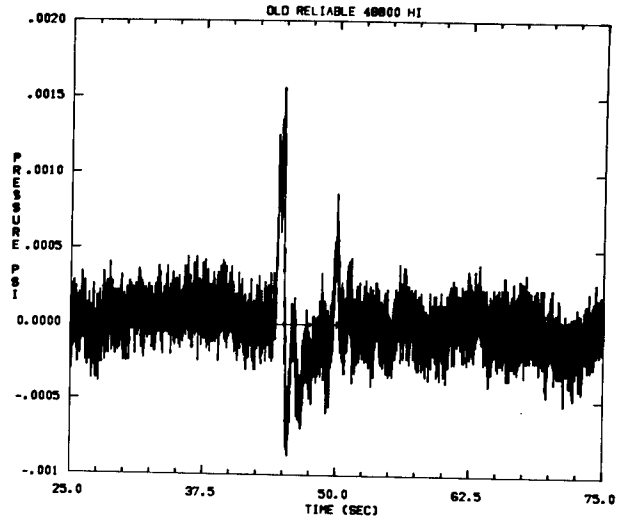

A= .000539168

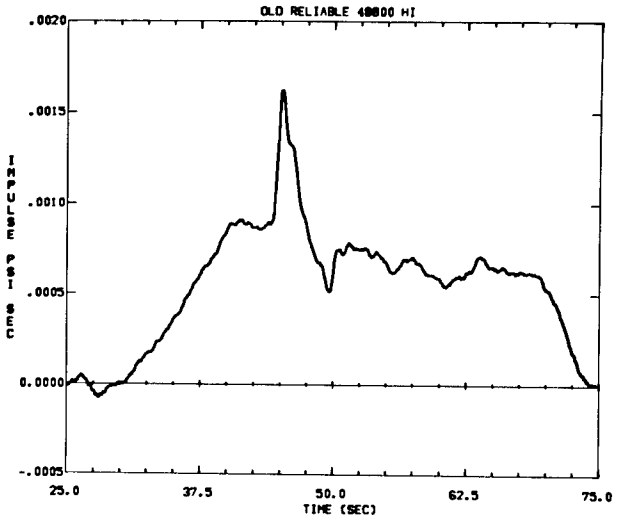

A= .000539168

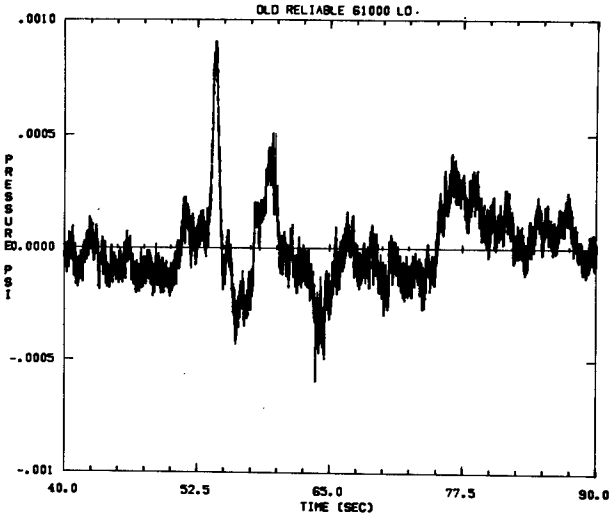

A= -.00033830

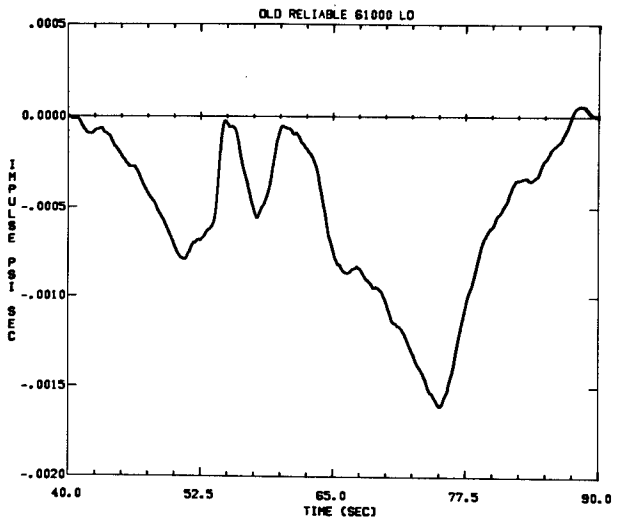

A= -.00033830

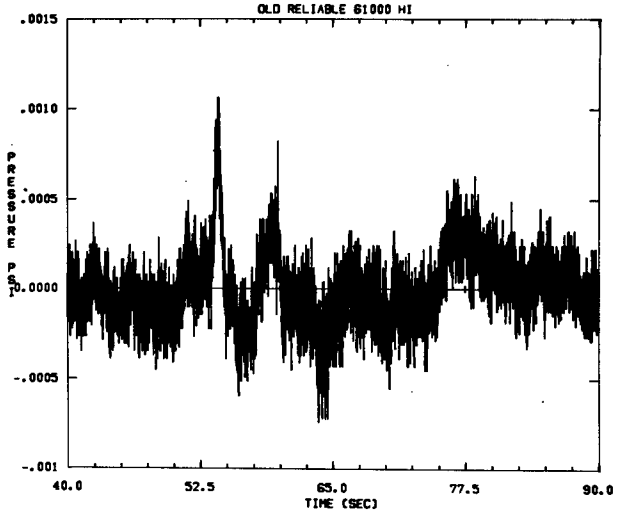

A= -.00026850

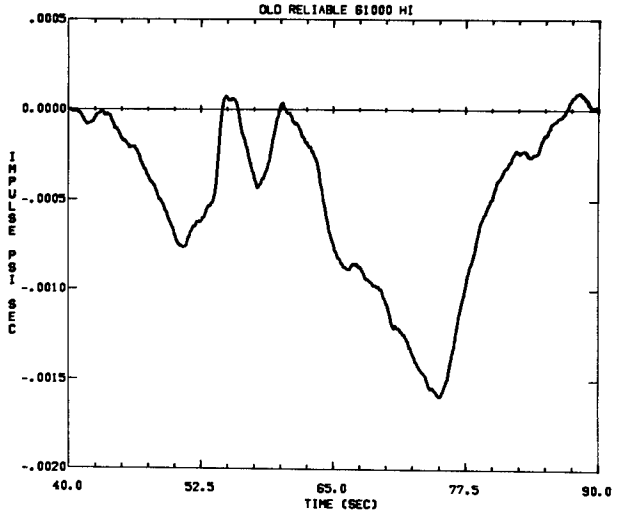

A= -.00026850

APPENDIX B

Plots of Pressure-Time, Impulse-Time and Energy Flux-Time after Records had been Processed to Remove Wind Noise and Electrical Noise

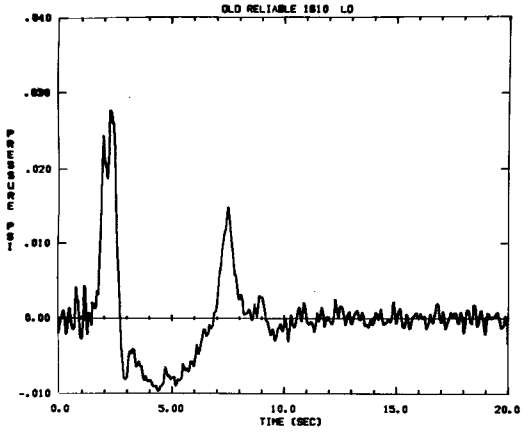

SMOOTHED3

A= -.00087105

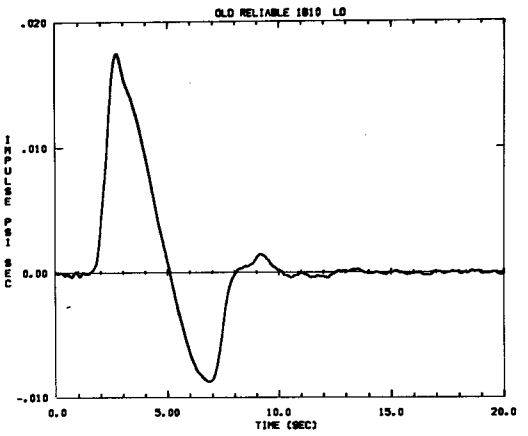

SMOOTHED3

A= -.00087105

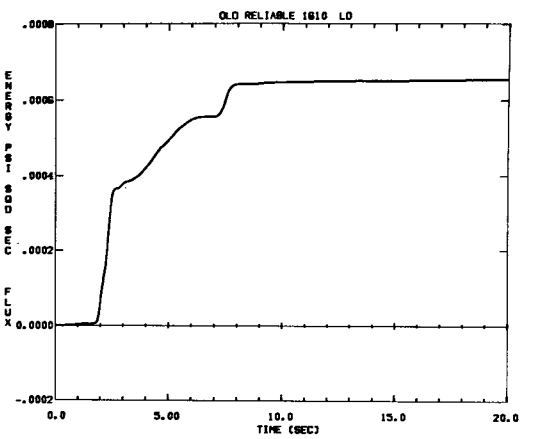

SMOOTHED

A= -.00087105

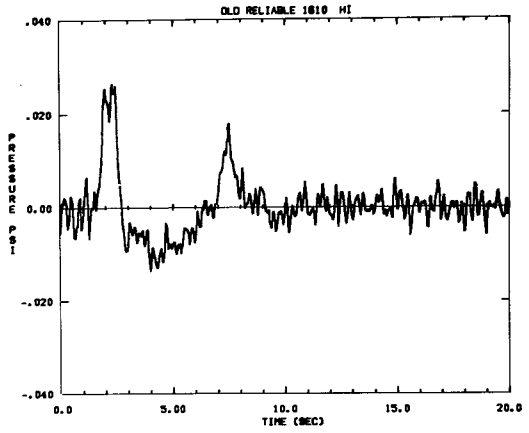

SMOOTHED3

A= -.00081579

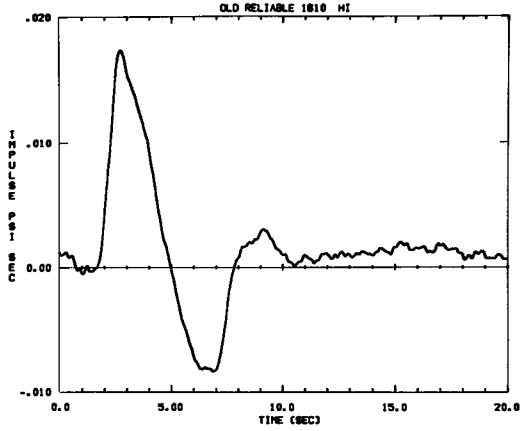

SMOOTHED3

A= -.00081579

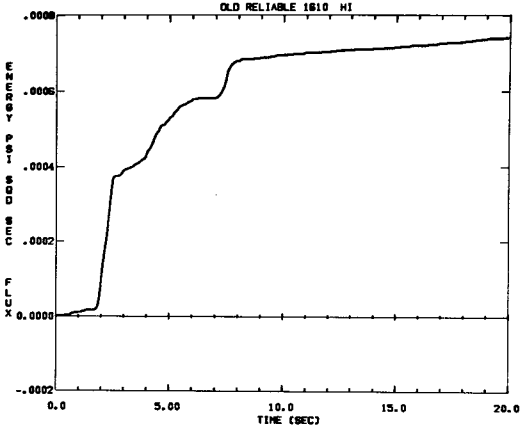

SMOOTHED

A= -.00081579

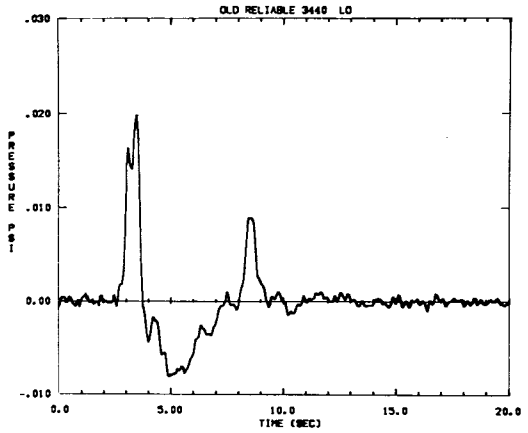

SMOOTHED3

A=.000221000

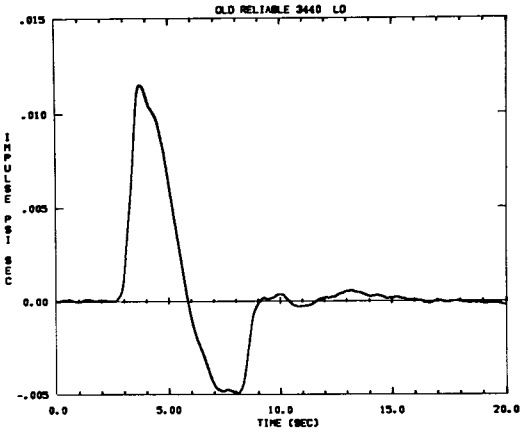

SMOOTHED3

A=.000221000

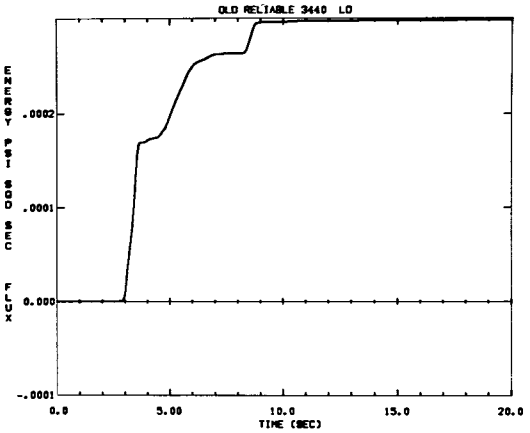

SMOOTHED

A=.000221000

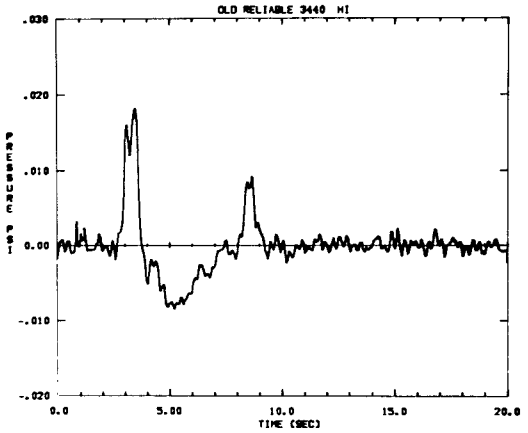

SMOOTHED3

A=.000384000

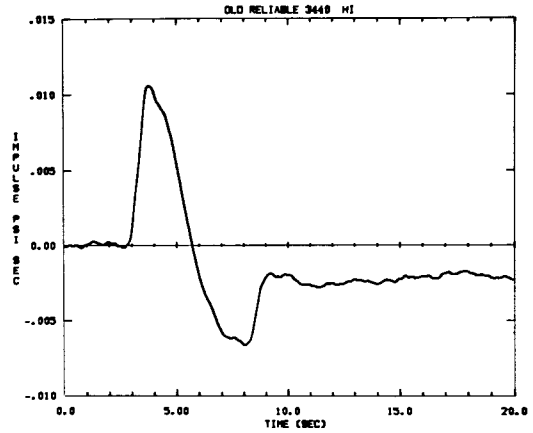

SMOOTHED3

A=.000384000

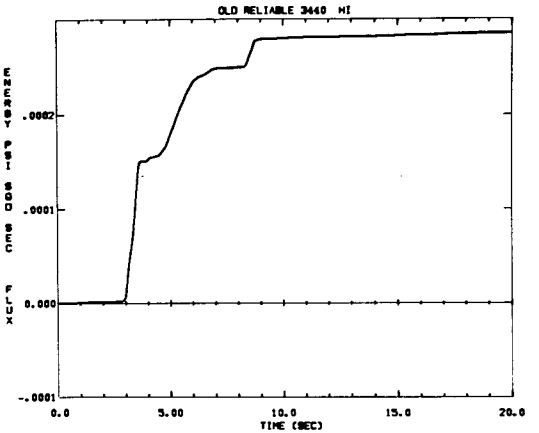

SMOOTHED

A=.000384000

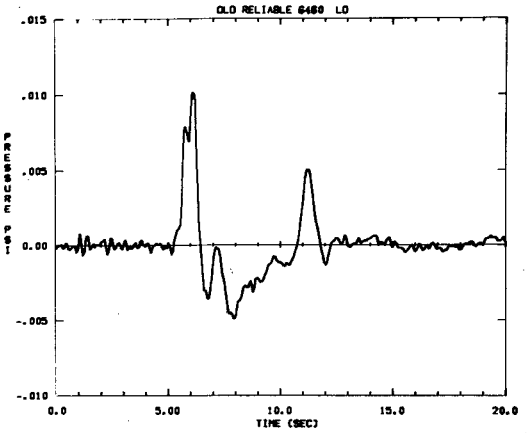

SMOOTHED3

A= -.00001101

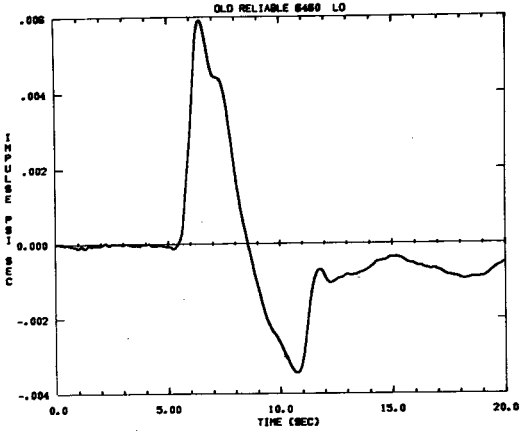

SMOOTHED3

A= -.00001101

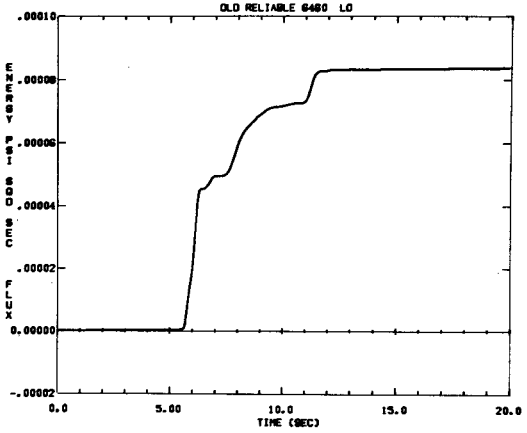

SMOOTHED

A= -.00001101

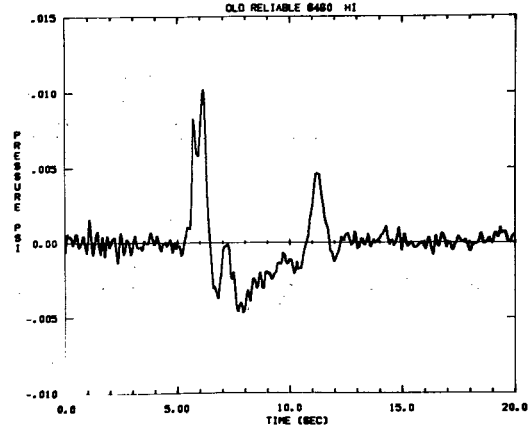

SMOOTHED3

A= -.00003846

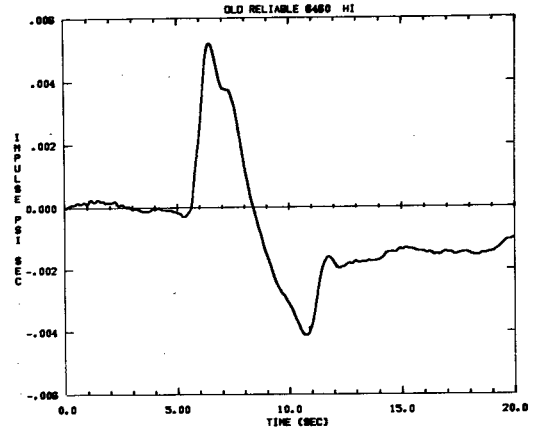

SMOOTHED3

A= -.00003846

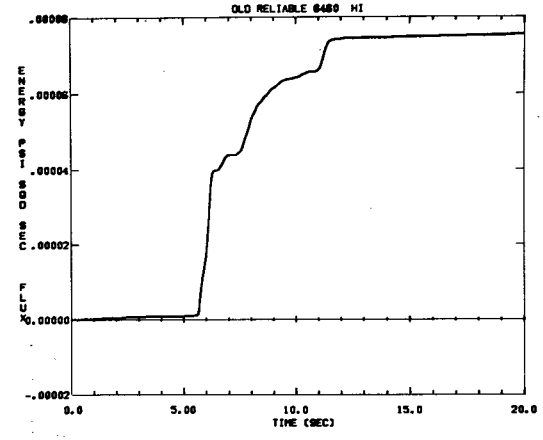

SMOOTHED

A= -.00003846

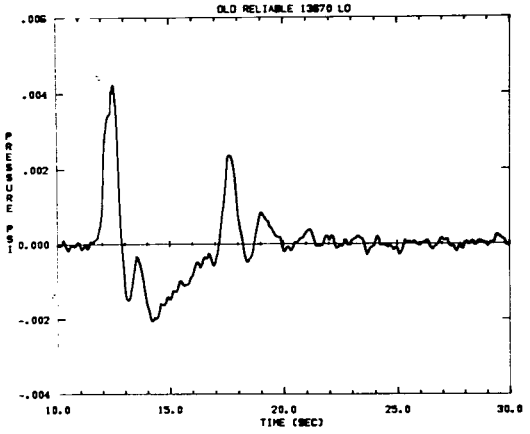

SMOOTHED3

A= -.00008787

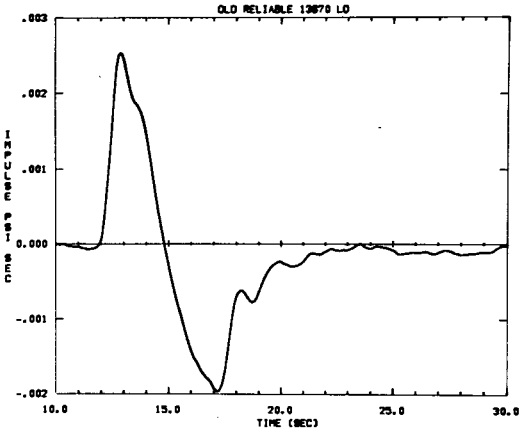

SMOOTHED3

A= -.00008787

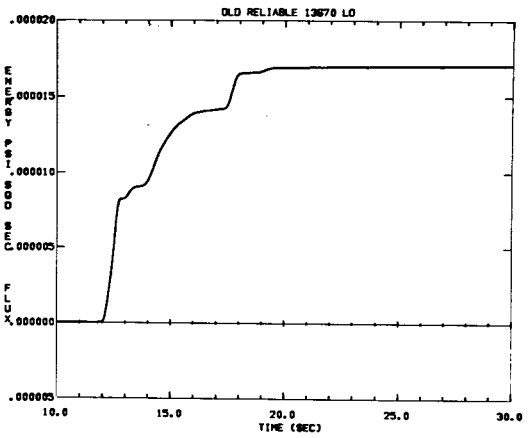

SMOOTHED

A= -.00008787

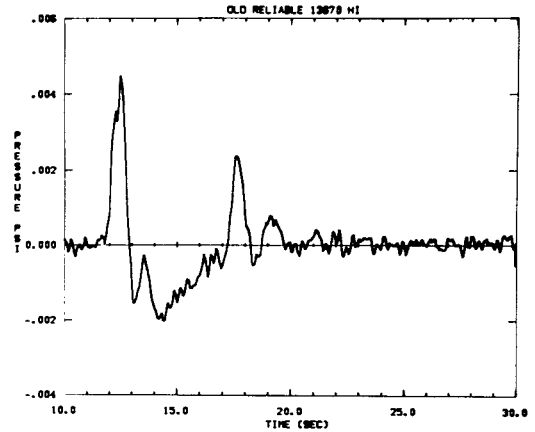

SMOOTHED3

A= -.00008863

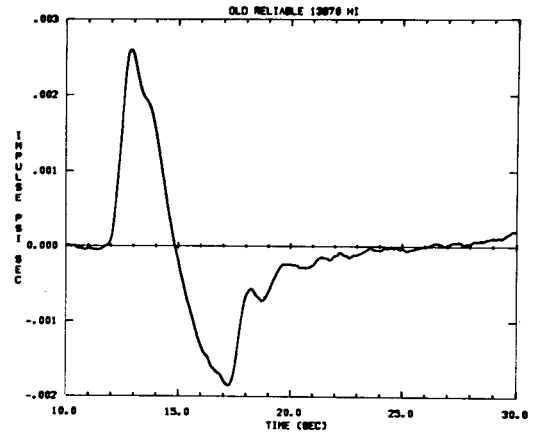

SMOOTHED3

A= -.00008863

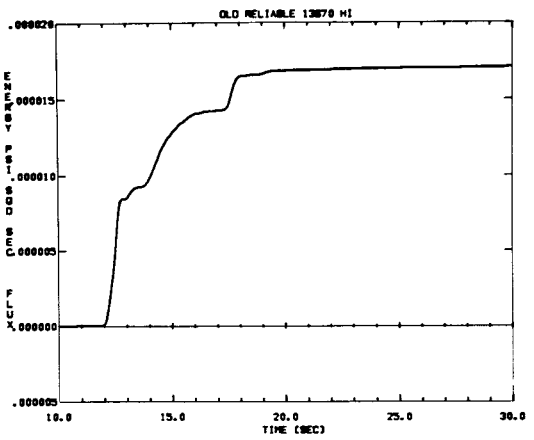

SMOOTHED

A= -.00008863

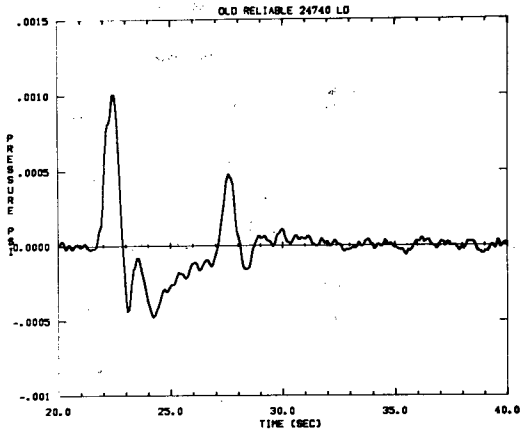

SMOOTHED3

A=.000006513

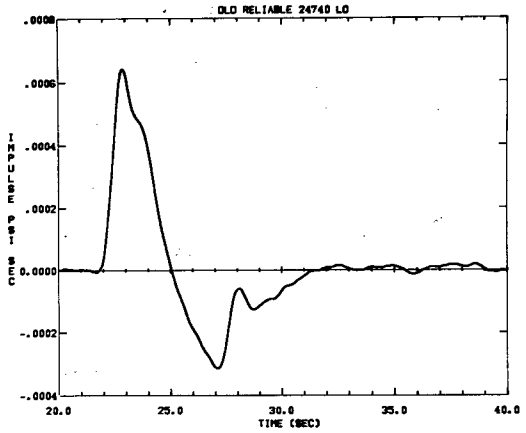

SMOOTHED3

A=.000006513

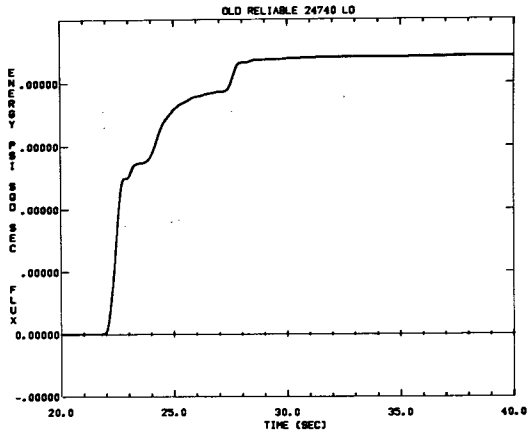

SMOOTHED

A=.000006513

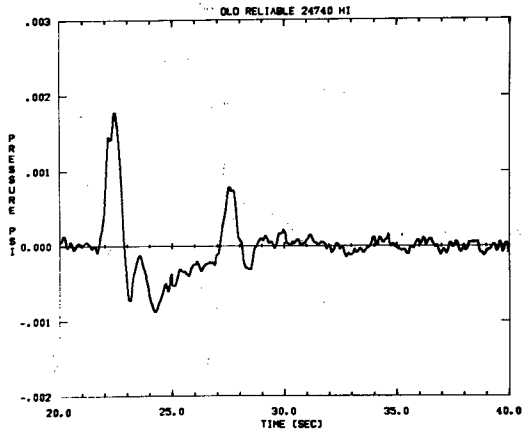

SMOOTHED3

A=.000039086

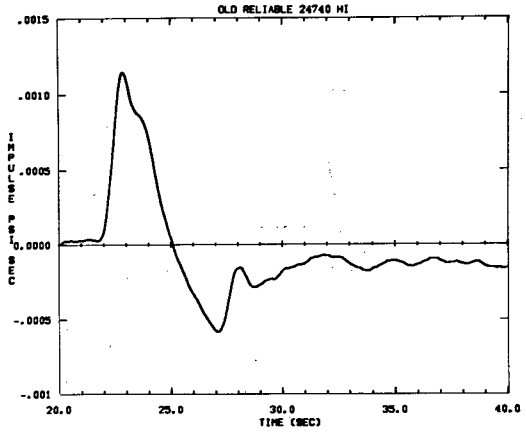

SMOOTHED3

A=.000039086

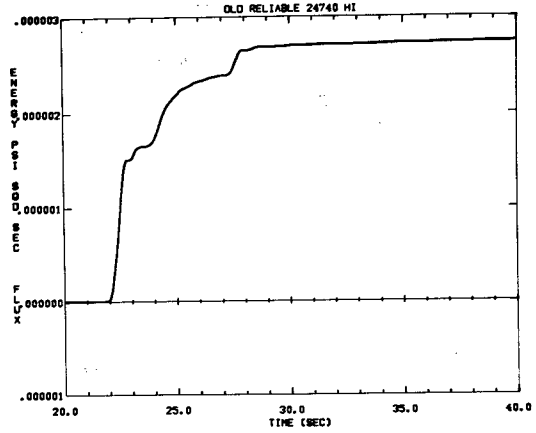

SMOOTHED

A=.000039086

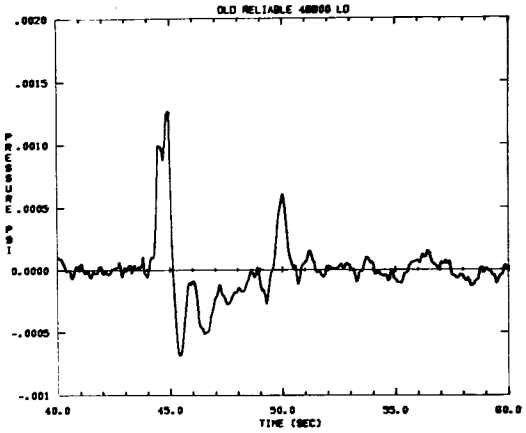

SMOOTHED3

A= -.00000478

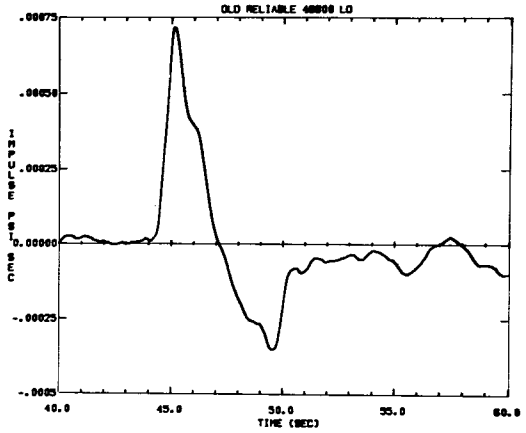

SMOOTHED3

A= -.00000478

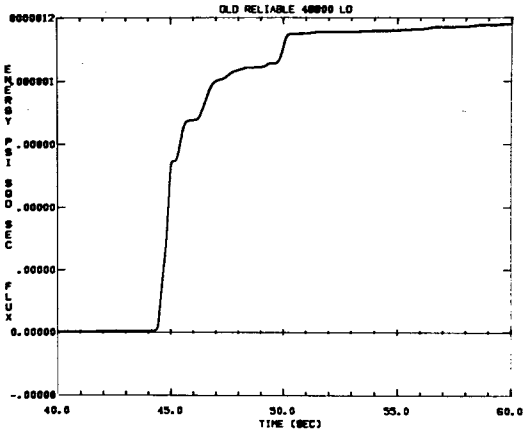

SMOOTHED

A= -.00000478

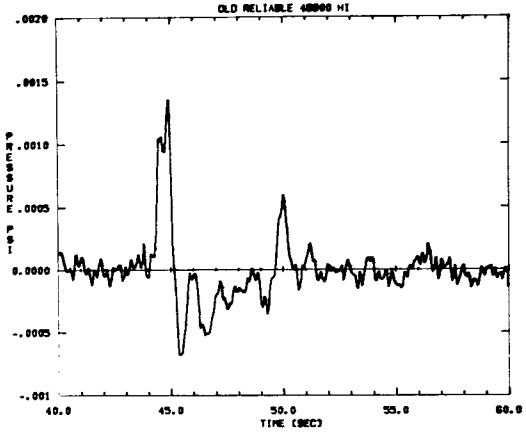

SMOOTHED3

A= -.00002737

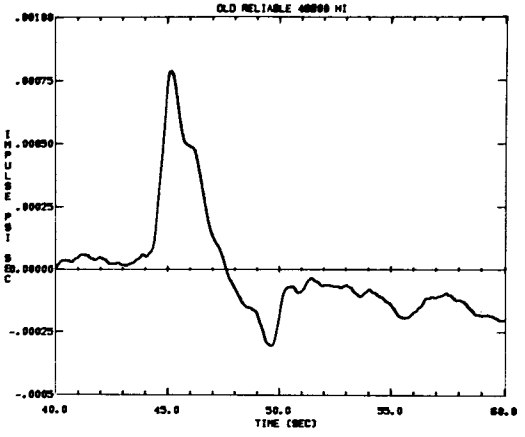

SMOOTHED3

A= -.00002737

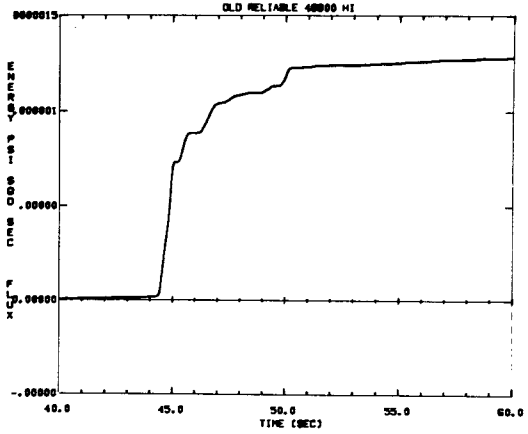

SMOOTHED

A= -.00002737

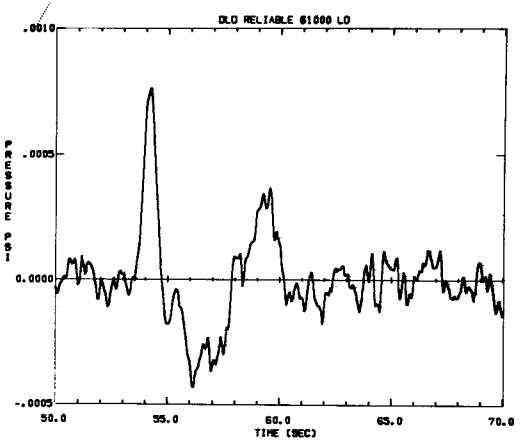

SMOOTHED3

A=.000017048

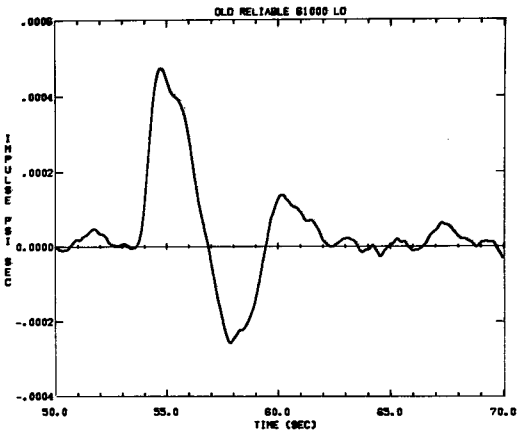

SMOOTHED3

A=.000017048

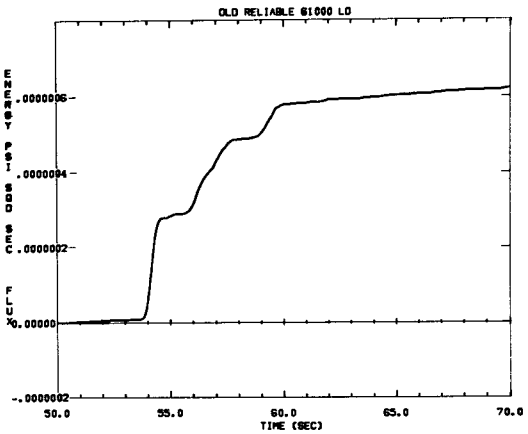

SMOOTHED

A=.000017048

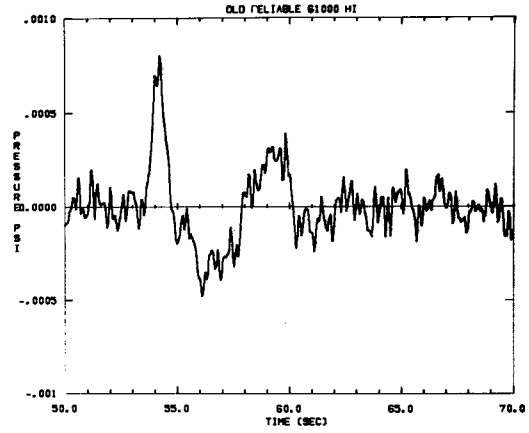

SMOOTHED3

A=.000017585

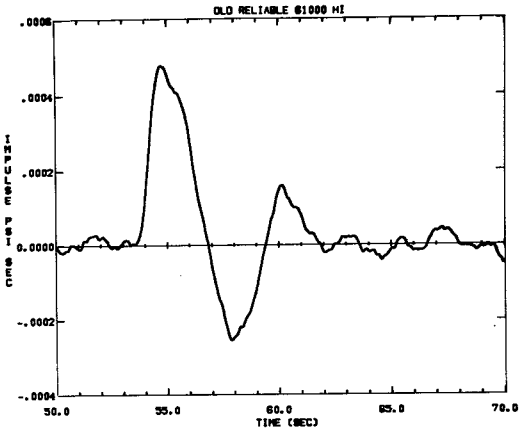

SMOOTHED3

A=.000017585

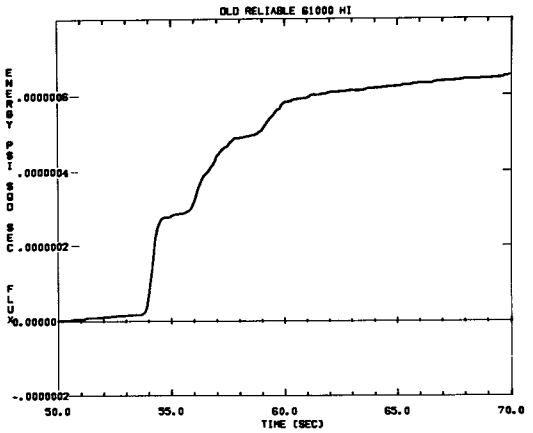

SMOOTHED

A=.000017585

DISTRIBUTION:

TID-4500, UC-35 (59th Ed.) (240)

Maj. Gen. Frank A. Cam
Asst. General Manager for
Military Application
U. S. Atomic Energy Commission
Washington, D. C. 20545

U. S. Atomic Energy Commission (5)
Division of Applied Technology
Washington, D. C. 20545
Attn: G. W. Johnson (2)
R. Hamburger
W. Oakley
J. Bresee

U. S. Atomic Energy Commission (2)
Albuquerque Operations Office
P. O. Box 5400
Albuquerque, New Mexico 87115

ESSA
Boulder Laboratories
Boulder, Colorado 80302
Attn: J. Rinehardt

The Boeing Company
P. O. Box 3999
Seattle, Washington 98124
Attn: R. H. Carlson 2-1770
Mail Stop 8A-38

Chief
Administrative Services Branch
Defense Atomic Support Agency
Washington, D. C. 20305
Attn: J. Kelso

U. S. Bureau of Mines (2)
Denver Mining Research Center
Bldg. 20 Denver Federal Center
Denver, Colorado 80225
Attn: P. L. Russell
Research Director

Los Alamos Scientific Laboratory (2)
P. O. Box 1663
Los Alamos, New Mexico 87544
Attn: J. C. Mark
W. E. Ogle

Stanford University
School of Engineering
Dept. of Civil Engineering
Stanford, California
Attn: Dr. P. Kruger 94305

M. A. Cook
Explosives Research Group
University of Utah
Salt Lake City, Utah 84112

U. S. Army Ballistic Research Lab
Aberdeen Proving Ground
Maryland 21005
Attn: J. J. Meszaros

Union Carbide Corp.
Nuclear Division
X-10 Laboratory Records Dept.
P. O. Box X
Oak Ridge, Tennessee 37830
Attn: W. E. Clark

R. M. Stewart
Director Mining Research
The Anaconda Company
1849 W. North Temple
Salt Lake City, Utah 84116

General Electric Co.
TEMCO
Center for Advanced Studies
816 State Street
Santa Barbara, California 93101
Attn: G. M. Crain

Michael R. Dence
Division of Gravity
Department of Energy, Mines and
Resources
Ottawa 3, Ontario, Canada

Chief, Special Projects Branch (2)
Geologic Division
U. S. Geologic Survey
Federal Center
Denver, Colorado 80225

Nuclear Group
E. Paso National Gas Company
El Paso, Texas 79999

Livermore Lawrence Laboratory (6)
P. O. Box 808
Livermore, California 94550
Attn: M. M. May
A. Holzer
J. B. Knox
M. D. Nordyke
J. Toman
G. C. Werth

Commanding Officer
Naval Weapons Evaluation Facility (SW)
Kirtland AFB
Albuquerque, New Mexico 87117

DISTRIBUTION (cont)

Commanding Officer
Air Force Weapons Laboratory
Attn: R. W. Henny/WLDC
Kirtland AFB
Albuquerque, New Mexico 87117

Mr. Robert M. Hannholm, Chief
Library and Archives Branches
U. S. Army Engineer School Library
Bldg. 270
Attn: Publications
Fort Belvoir, Virginia 22060

Defense Documentation Center
Alexandria, Virginia 22313

U. S. Army Engineer Nuclear
Cratering Group (2)
Livermore, California 94550

Director
U. S. Army Engineers
Waterways Experiment Station
Vicksburg, Miss. 39180

E. I. DuPont de Nemours & Co.
Potomac River Laboratory
Martinsburg, W. Virginia
Attn: D. D. Porter

E. I. DuPont de Nemours & Co. (2)
Experimental Station
Wilmington, Delaware 19898
Attn: A. B. Andrews
D. W. Carey

Ranchers Exploration and Development Corp. (2)
Albuquerque, New Mexico
Attn: A. G. Miller
D. K. Hogan

William Elliot
Magma Copper Co.
San Manuel Division
San Manuel, Arizona 85631

J. A. Hornbeck, 1
T. B. Cook, 8000
C. S. Selvage, 8180
G. A. Fowler, 9000
C. F. Bild, 9100
C. D. Broyles, 9100
J. D. Kennedy, 9110 (10)
W. D. Weart, 9111
G. E. Hansche, 9120
J. R. Dickinson, 9123
H. E. Viney, 9130
J. R. Banister, 9150
W. L. Holley, 9150
J. W. Reed, 5644
L. S. Ostrander, 8232
L. C. Baldwin, 3152
Technical Publications Division I, 3151 (3)
for: AEC/TIC
Central Files, 3148-2 (15